5. Nitrous Oxide and Halocompounds

J.W. ELKINS (EDITOR), J.H. BUTLER, T.M. THOMPSON, S.A. MONTZKA, R.C. MYERS, J.M. LOBERT, S.A. YVON, P.R. WAMSLEY, F.L. MOORE, J.M. GILLIGAN, D.F. HURST (WITH CCG), A.D. CLARKE, T.H. SWANSON, C.M. VOLK, L. T. LOCK, L.S. GELLER (WITH CCG), G.S. DUTTON, R.M. DUNN, M.F. DICORLETO, T.J. BARING, AND A.H. HAYDEN

5.1. CONTINUING PROGRAMS

5.1.1. INTRODUCTION

The Nitrous Oxide and Halocarbons Group was formed in 1986. In April 1995, the name was changed to Nitrous Oxide and Halocompounds Group (NOAH) to reflect the fact that noncarbon containing, halogenated gases such as sulfur hexafluoride (SF_6) are now an integral part of our program. The general mission of the group is to quantify the distributions as well as the magnitudes of the sources and sinks for atmospheric nitrous oxide (N_2O) and halocarbons that include the chlorofluorocarbons (CFCs), chlorinated solvents (CCl_4, CH_3CCl_3, etc.), hydrochlorofluorocarbons (HCFCs), hydrofluorocarbons (HFCs), methyl halides (CH_3Br, CH_3Cl, CH_3I), halons, and numerous other important ozone-depleting and greenhouse gases. Two chromatographic techniques, electron capture detector-gas chromatography (EC-GC) and gas chromatograph-mass spectrometer (GC-MS), are used primarily to detect these trace atmospheric species. NOAH samples air from ground-based stations, towers, ocean vessels, aircraft, and balloons to accomplish its mission. Achieving these goals requires the production and maintenance of reliable gas calibration standards that are supplied to laboratories throughout the world.

New sites for both the flask and in situ programs were added over the past 2 years. The location of these sites in the CMDL N_2O and Halocompounds Network are shown in Figure 5.1. In cooperation with the Carbon Cycle Group (CCG), two tower sites (WITN Tower, North Carolina (ITN) and WLEF Tower, Wisconsin (LEF)) were added to the in situ program to ascertain source strengths of gases near urban and forested areas. With a similar purpose, an in situ gas chromatograph (GC) system was started at Harvard Forest (HFM) in collaboration with Harvard University scientists. At Alert, Northwest Territories, Canada (ALT) and in cooperation with the Canadian Atmospheric Environment Services (AES) program, an in situ GC for measuring N_2O and SF_6 also was installed and operated in 1995. Monthly, and in some cases weekly, flask samples were collected at these new in situ sites. Another site within CMDL, Cape Kumakahi, Hawaii (KUM), was added to obtain flask measurements of air from the remote, tropical, northern hemispheric marine boundary layer. Combined with MLO, this should allow us to estimate vertical gradients of trace atmospheric halocarbons, particularly those that react readily with sunlight or tropospheric OH. Table 5.1 summarizes the geographic location and type of operations of eleven flask and nine in situ sampling sites.

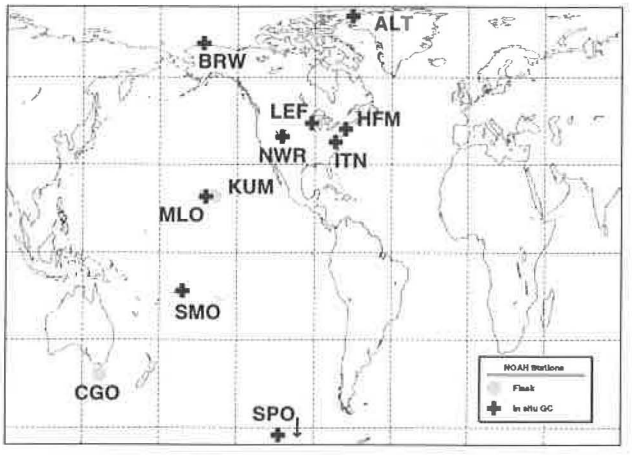

Fig. 5.1. Geographical locations of old and new stations in the NOAH flask (gray circles) and in situ (pluses) networks.

5.1.2. FLASK SAMPLES

Overview

NOAH's flask sampling and measurement program underwent a number of changes and improvements in 1994 and 1995. Most significant of these was the retirement of the "old" flask GC, a Hewlett-Packard (HP) Model 5710A GC-ECD, at the end of 1995 used for the measurement of CFC-12 (CCl_2F_2), CFC-11 (CCl_3F), and N_2O since inception of the old GMCC halocarbon monitoring program in 1973. This instrument, which operated in an almost entirely manual mode and for which data reduction was a cumbersome process, was replaced by the NOAH automated flask GC (OTTO). The OTTO GC, which began operation in 1992, analyzes samples for seven gases. A detailed comparison of mixing ratios of CFC-11, CFC-12, and N_2O from all stations between the old HP 5710A and OTTO GCs shows that the new OTTO GC gives better precision and close agreement with the older GC (Figure 5.2). The Whitey 300 mL-flasks were also removed from the sampling network. Over the past 10 years, the flask network was augmented with increasingly large flasks (0.85 L and 2.4 L) to accommodate the increased number of measurements and larger amounts of air required. The last Whitey flasks were filled at the end of 1995 at all stations except at the South Pole Observatory, Antarctica (SPO), which will not be able to return them until its reopening in the fall of 1996. Originally selected for sampling of stable CFCs and N_2O, the Whitey flasks, with their smaller volume and coarser internal surfaces, were also increasingly problematic for some of the more reactive gases such as methyl chloroform (CH_3CCl_3), carbon tetrachloride (CCl_4), and methyl bromide (CH_3Br) that were added to the suite of measurements over time. All flasks in the network are now 0.85-L Biospherics or 2.4-L Max Planck Institute (MPI) electropolished, stainless steel containers with Nupro metal-bellows (SS-4H) valves.

TABLE 5.1. Geographic and Network Information on NOAH Network Sites (In Order of Highest Latitude)

Code	Station	Latitude	Longitude	Elevations (m)	LST-GMT (hr)	Type
ALT	Alert, North West Territories. Canada*	82.45°N	62.52°W	210	-4	F,I
BRW	Pt. Barrow, Alaska	71.32°N	136.60°W	11	-9	F,I
LEF	WLEF tower, Wisconsin†	45.95°N	90.28°W	470	-6	F,I
HFM	Harvard Forest, Massachusetts‡	42.54°N	72.18°W	340	-5	F,I
NWR	Niwot Ridge, Colorado§	40.04°N	105.54°W	3013	-7	F,I
ITN	WITN tower, North Carolina†	35.37°N	77.39°W	9	-5	F,I
MLO	Mauna Loa, Hawaii	19.54°N	155.58°W	3397	-10	F,I
KUM	Cape Kumukahi, Hawaii	19.52°N	154.82°W	3	-10	F
SMO	Tuluila, American Samoa	14.23°S	170.56°W	77	-11	F,I
CGO	Cape Grim, Tasmania, Australia**	40.41°S	144.64°E	94	+10	F
SPO	South Pole, Antarctica	89.98°S	102.00°E	2841	+12	F,I

Cooperative sites (F = flasks, I = in situ) with:

*AES, in situ GC: Only N_2O and SF_6

†CCG. Flasks will be added to WLEF in 1996. The ACATS-II instrument ran as an in situ GC at WLEF for 1995.

‡Harvard University

§University of Colorado

**Commonwealth Scientific and Industrial Research Organization (CSIRO) and Bureau of Meteorology, Australia

Flasks are now filled to 376-505 kPa (40-60 psig) at all sites. Although this typically has not been a problem at sea level where the KNF Neuberger, Inc. pumps (Model UN05SV1) are rated to deliver 410 kPa (45 psi), samples collected at higher altitudes (SPO, Mauna Loa Observatory, Hawaii (MLO), Niwot Ridge, Colorado (NWR)) could only reach pressures around 273 kPa (25 psig), which today are barely enough gas for CMDL measurements. To accommodate this change, the inlets were reconfigured to the automated, in situ GCs to allow the Neuberger pumps to draw air from the pressurized portion of the inlet line. Although the inlet lines (Dekabon) and pumps (Air-Cadet, Cole-Palmer) contain plastic, they are kept clean by continuous flushing, 24 hours per day at 5-10 L min^{-1}. No noticeable difference was observed in the data as a result of making this change. Pumps and lines have been installed at NOAA sites, e.g., KUM, that do not support in situ GCs.

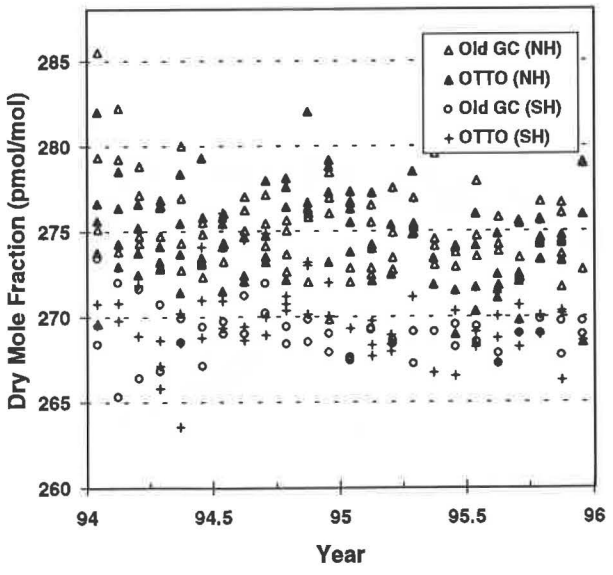

Fig. 5.2. Continuity of CFC-11 data from the old GC and automated flask GC (OTTO) during 1994-1995. Data are shown for sites in both hemispheres.

In addition to the routine, weekly sampling of flask pairs at the CMDL observatories and cooperative sampling sites, NOAH scientists also analyzed air in flasks collected during two cruises in 1994 (Bromine Latitudinal Air/Sea Transect (BLAST I and BLAST II); section 5.4 and SF_6 section) to obtain "snapshots" of the interhemispheric gradient of a number of gases and to support measurements made by in situ GCs onboard. These measurements included over 25 gases and involved all of NOAH laboratory instrumentation. Another project (section 5.6) involved the flask program for the analysis of air sampled from South Pole firn (compressed snow). This provided NOAH scientists with a unique opportunity to observe the N_2O and halocarbon content of air dating back to the end of the 19th century. Although the air was collected into glass flasks with Teflon o-rings, which in the past have caused some problems in the analysis of halocarbons, contamination was minimal for most gases in this instance. The success of these measurements prompted NOAH scientists to pursue similar analyses from firn air collected at Vostok and Greenland. Because of the number of investigators requiring air from the SPO flasks, sharing was limited. Consequently, the samples were analyzed only with the OTTO and Low Electron Attachment Potential Species (LEAPS) GCs, which require less sample than the GC-MS systems.

Finally, a number of changes were made in instrumentation, data acquisition, and data management for flask measurements that have improved the precision of some measurements, enhanced detection limits for others, and dramatically streamlined the processing of data. Today, data from samples run on OTTO and LEAPS can be

finalized and evaluated alongside all previous data within minutes following analysis.

Measurements by EC-GC

Improvements in Analysis. The precision of flask measurements by EC-GC has improved dramatically during 1994-1995. Modifications in sampling technique and sample introduction, full automation of CFC, N_2O, and chlorocarbon measurements, and installation of 24-bit interfaces for analyses by OTTO and LEAPS combined to yield analytical and sampling precisions about 0.1 ppt or less for LEAPS gases and on the order of tenths of a ppt for gases measured on OTTO.

The old Nelson Analytical, Inc. data acquisition and handling system on OTTO was replaced with entirely new hardware and software to allow more rapid and consistent processing of samples. The HP Model 210 computer was replaced with an IBM PC compatible 486, the 16-bit A/D converters were replaced with two HP 24-bit A/D boards for the PC, and the Rocky Mountain Basic software was replaced with the 1995 version of HP Chemstation software. Programs were written in Microsoft Visual Basic to consolidate the HP Chemstation output from each run of flasks, compute results, generate flags for erroneous or anomalous data, perform additional quality control tests, and load the results into a Microsoft Access data base. Currently, eight flasks can be run at once on OTTO, obtaining precise measurements of CFC-12, CFC-11, CFC-113, CH_3CCl_3, CCl_4, N_2O, and SF_6.

Results and Trends. The years 1994 and 1995 heralded the downturn in total chlorine, equivalent chlorine, and effective equivalent chlorine in the earth's troposphere [*Montzka et al.*, 1995b, 1996b]. Led by a marked drop in CH_3CCl_3, this suggested that the abundance of ozone-depleting halogen in the stratosphere could begin to decline in the near future. Other gases that began decreasing in abundance during this time include CFC-113, CCl_4, and, to a lesser extent CFC-11 (Figure 5.3). CFC-12 continued to increase in the atmosphere, although not in sufficient quantity to offset the losses in organic chlorine represented by the other compounds (Figure 5.3). As expected, the atmospheric abundances of CFC alternative compounds (HCFCs and HFCs) have been increasing at reasonably fast rates, although these gases contain relatively little chlorine and have shorter lifetimes than the CFCs ([*Montzka et al.*, 1993, 1994, 1996a,b]; section 5.1.5).

SF_6—An Important Tracer and Strong Greenhouse Gas

On a per molecule basis, SF_6 is one of the strongest greenhouse gases known, about 25,000 times greater than CO_2 [*Albritton et al.*, 1995]. It is solely anthropogenic in origin and used primarily for the insulation of high-voltage electrical equipment. With its increasing use and very long

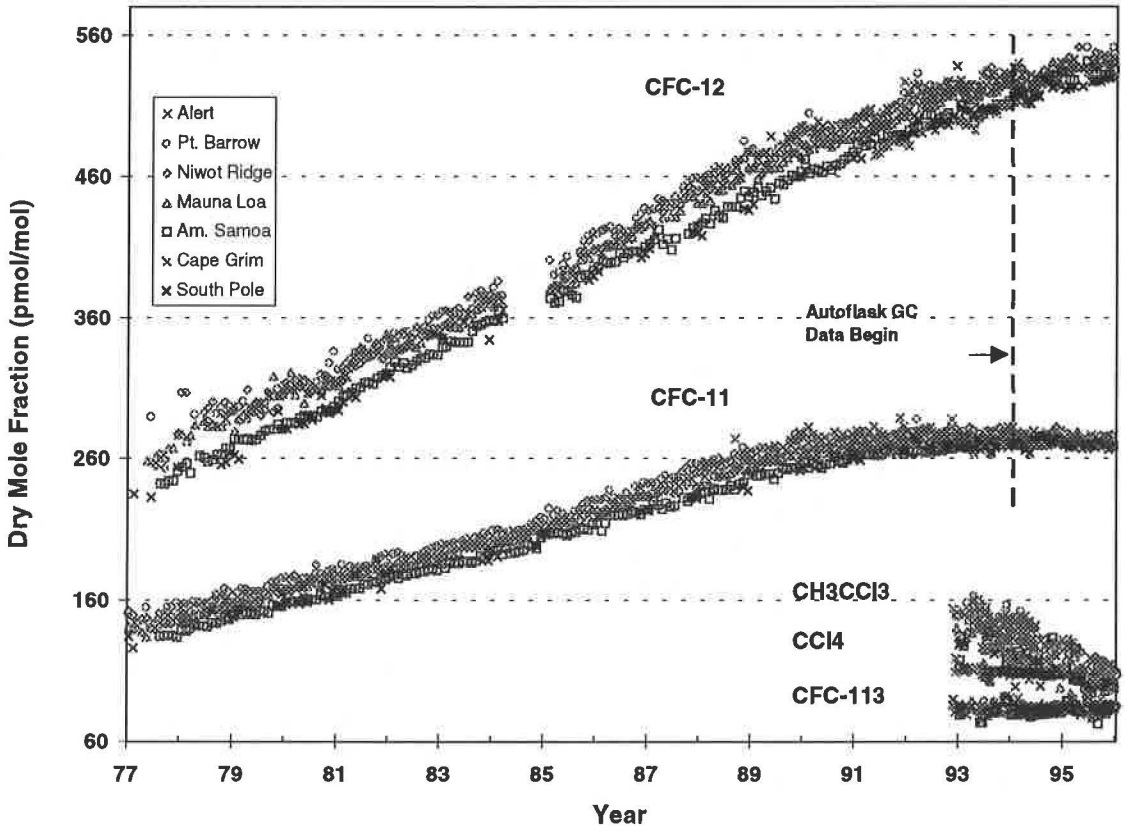

Fig. 5.3. CFCs and chlorocarbons measured on the old GC and OTTO in ppt versus time since 1977. The transition from old GC data to OTTO data for CFCs -11 and -12 is shown by a vertical, dashed line at the beginning of 1994. Noticeable are the tighter measurements of OTTO and the lack of an offset between the instruments. Also shown in proportion are the recent growth rates of the major, Class I ozone-depleting, chlorinated compounds and their narrowing interhemispheric gradients.

lifetime, SF_6 is rapidly accumulating in the atmosphere at ~7% yr^{-1}. In addition to its importance as a greenhouse gas, SF_6 is a nearly ideal tracer of atmospheric dynamics due to its well understood sources and long atmospheric lifetime of ~3200 years [*Ravishankara et al.*, 1993].

CMDL scientists recently began monitoring atmospheric SF_6 in weekly flask samples from all baseline stations and many CCG network sites as high-resolution latitudinal profiles during the 1994 BLAST ocean cruises [*Geller et al.*, 1994] as in situ stratospheric measurements from the Airborne Chromatograph for Atmospheric Tracers (ACATS) field missions [*Elkins et al.*, 1996], and as in situ measurements at Alert, Harvard Forest, and North Carolina [*Hurst et al.*, 1995]. SF_6 was measured with ECD-GC as described in *Elkins et al.* [1996]. Even though ambient levels of SF_6 are only ~3.5 ppt, it is possible to measure direct air injections (no sample preconcentration) to a precision of 1-3%. A suite of gravimetric SF_6 standards ranging from 3 to 108 ppt was developed in the NOAH Group. An intercalibration with the University of Heidelberg (Germany) showed CMDL measurements are less than 2% lower that the German calibration scale.

The long-term trend of SF_6 is illustrated in Figure 5.4, which shows NOAA data together with the University of Heidelberg data. These different data sets, collected and analyzed by different techniques, show good agreement. A northern hemispheric trend was fit to the combined Izaña and NWR data, because data from these two midlatitude sites are close to the latitudinally weighted hemispheric mean. Likewise, in the southern hemisphere, data from Antarctica and Cape Grim well represent the true southern hemisphere mean, therefore the southern hemisphere trend was fit to the Neumayer and Cape Grim data from the University of Heidelberg, and the SPO and Cape grim data from NOAA data. A preliminary estimate for the global trend (the average of the northern and southern hemispheric trends) shows a quadratic increase described by: $y = 3.43 - 0.2352 \times + 0.00487x^2$ (for x = (year - 1996); 0.23 ppt yr^{-1} (6.86% yr^{-1}). This trend, which is derived from the combined data sets, shows no significant difference from the trend derived from the University of Heidelberg data alone [*Maiss et al.*, 1996]. Figure 5.5 shows the high resolution latitudinal profiles of SF_6 collected over both the Pacific and Atlantic oceans on the BLAST cruises of 1994. Figure 5.5c also shows a mean latitudinal profile of SF_6 for November 1995 obtained from the flask sampling network. These profiles should not be taken as representative of an overall global distribution of SF_6 since they can vary seasonally.

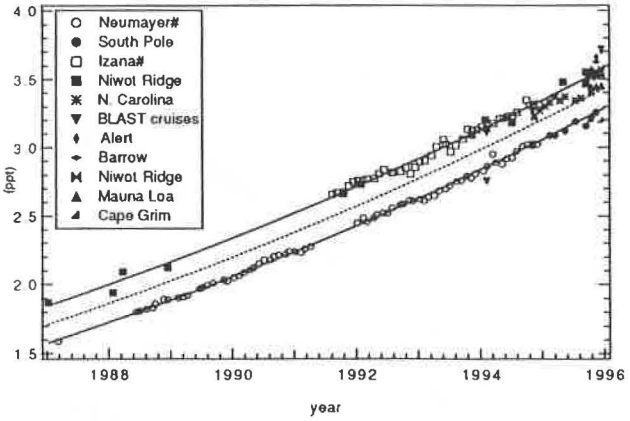

Fig. 5.4. Temporal trends of SF_6. CMDL data shown together with University of Heidelberg data [from *Maiss et al.*, 1996, marked in the figure legend as #]. The Heidelberg data has been adjusted to the CMDL calibration scale and binned into monthly means. The curve fitting is described in the text.

5.1.3. RITS Continuous Gas Chromatograph Systems

Operations Update

A new watchdog timer turns the power off, then resets the computer, printer, and Nelson A to D boxes if a signal 1987 < year <1996). This yields a late 1995 growth rate of by: $y = 3.43 - 0.2352 \times + 0.00487x^2$ (for x = (year - 1996);

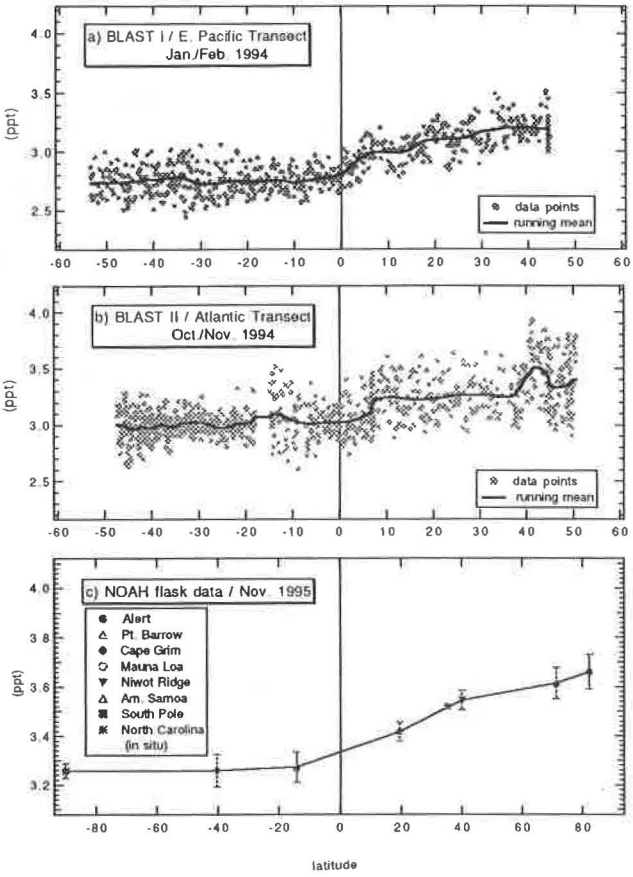

Fig. 5.5. Latitudinal profiles of atmospheric SF_6 (dry, ppt by mole fraction). (a) and (b) are in situ data from the marine boundary layer in 1994. (c) shows the monthly mean mixing ratios for November 1995 obtained from flask samples collected at seven sampling stations and from the in situ North Carolina data. Error bars represent ±1 standard deviation of the flask pair mixing ratios at each station.

is not received in a specified recurring period of time. This restarts data acquisition when station personnel are not present at night or on weekends and the system locks up. In June 1994 the hardware was installed at the Barrow Observatory, Alaska (BRW) in June and at MLO and Samoa Observatory, American Samoa (SMO) in August. At this same time a new function was added to the system software to decrease paper usage by the printer. A set of calibration gas and air chromatograms were printed only once a day prior to the arrival of the station personnel instead of continuous printouts. In August, system software was modified to include a menu-driven log for problems, failures, and changes to be easily documented. In the past such information was written on daily and weekly check lists and then typed into a database.

Original data acquisition and control computers, HP Model 9816s of mid-1980 vintage, were replaced in 1995 by 486 PCs. The software port from HP Basic to TransEra HTBasic running in Microsoft Windows 3.1 required only minor changes. This software upgrade was installed in April at NWR, in May at MLO and SMO, and in June at BRW. An additional feature of the new computers is network access. Data downloading, software upgrading, and determining equipment status is now possible over the Internet.

Alert

A single-channel GC equipped with an ECD and based on the STEALTH GC design (section 5.5) was built in 1995 and installed at ALT as part of a cooperative research agreement between CMDL and AES. Continuous instrument operation began in late August 1995 with two samples of ambient air analyzed each hour for N_2O and SF_6. These measurements augment the weekly flask samples taken at ALT since late 1987 and allowed detection of episodic pollution events. Of particular interest was the monitoring of polluted air that arrives at Alert from northern Asia and from the former Soviet Union.

Data Analysis

In response to observed depletion of stratospheric ozone, the 1987 Montreal Protocol on Substances That Deplete the Ozone Layer mandated a 50% reduction of chlorofluorocarbons and selected chlorinated solvent production over the next 10 years. In 1990 this was strengthened to a 100% phase out by the year 2000. An additional amendment in 1992 required a 75% reduction by 1994 and a complete ban by 1996. The chemical industry responded quickly with substitutes. Emissions have, therefore, generally been reduced in excess of expectations.

The global average CFC-11 tropospheric mixing ratio reached a maximum of 272 ppt in 1993 (Figure 5.6). The growth rate has now started to decline at -1 ppt yr^{-1}. Recently the interhemispheric difference declined by half, indicative of a long lifetime and a mostly northern hemisphere source that is diminishing quickly. In situ measurements of CFC-11 and CFC-12 are described in *Elkins et al.* [1993], and the data were recently updated in *Montzka et al.* [1996b].

CFC-12 growth continues to slow down with the end of 1995 growth rate about 6 ppt yr^{-1}. Because CFC-12's major use is in domestic, commercial, and industrial

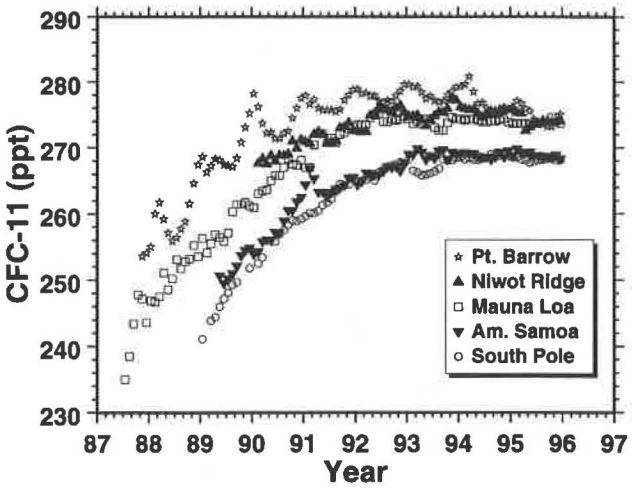

Fig. 5.6. Monthly average CFC-11 mixing ratios in ppt from the in situ GCs.

refrigeration and air conditioning, release to the atmosphere is slower than foam blowing, propellant, and solvent applications. Assuming a constant deceleration of -1.66 ppt yr^{-2}, CFC-12 is estimated to peak in the atmosphere in mid-1999 with a global-average tropospheric mixing ratio of 544 ppt (Figure 5.7 and 5.8).

Southern hemispheric mixing ratios of methyl chloroform peaked in 1992 and northern hemisphere mixing ratios peaked a little more than a year earlier (Figure 5.9). The time lag is similar to the known interhemispheric mixing time. The large north to south gradient before 1993 is indicative of very strong northern hemisphere sources. The rapid decrease in mixing ratios during phaseout shows the chemical has a short lifetime estimated at about 5 years [*Prinn et al.*, 1995].

The chlorinated solvent CCl_4, was used as the primary source (feed stock) for the chemical synthesis of all the chlorofluorocarbons. With their ban, this role has

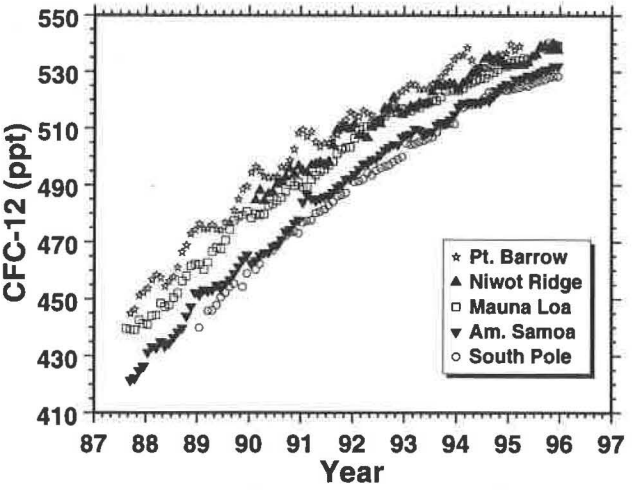

Fig. 5.7. Monthly average CFC-12 mixing ratios in ppt from the in situ GCs.

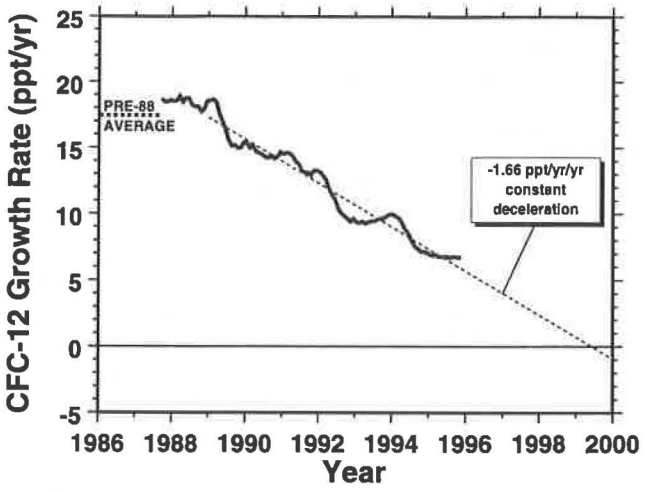

Fig. 5.8. A decrease in the global average growth rate of CFC-12 is projected to become zero in mid-1999.

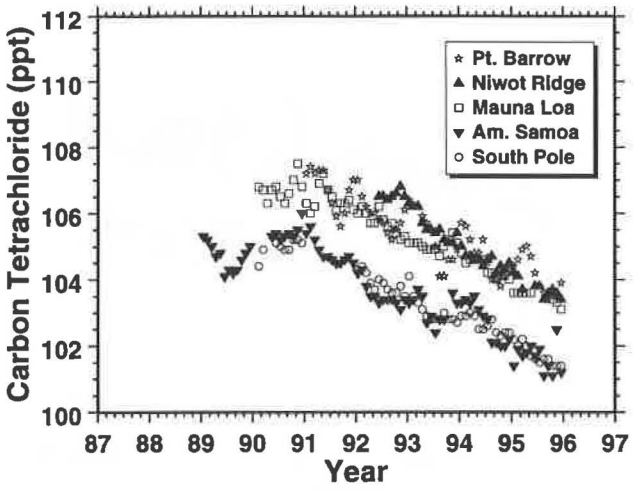

Fig. 5.10. Monthly average CCl_4 mixing ratios in ppt from the in situ GCs.

diminished significantly. Atmospheric mixing ratios were observed to be slowly decreasing at approximately -0.75 ppt yr^{-1} since 1991 (Figure 5.10). One unusual feature is the north to south gradient was near constant during this same period.

The methyl chloroform and carbon tetrachloride data were published in *Montzka et al.* [1996b]. The mixing ratios of both compounds are decreasing with time as a result of the Montreal Protocol.

N_2O continued to increase in the troposphere (Figure 5.11). The average global growth rate for 1995 was 0.61 ppb yr^{-1}.

5.1.4. LEAPS

Although precision of the Low Electron Attachment Potential Species (LEAPS) analyses was improved by an order of magnitude in 1992 with better chromatography (tenths to hundredths of a ppt; *Swanson et al.* [1993]; *Thompson et al.* [1994]), the system still operated with the old Nelson Analytical hardware and software. In 1994 this was replaced with a 24-bit A/D board and an IBM PC-compatible 386, and HP Chemstation software. New software was written for processing data and incorporating it into a Microsoft Access data base manager. As with data from OTTO, final LEAPS data are now available immediately following analysis.

Halons have not been produced by industry since January 1, 1994, except for some small exceptions; however, the mixing ratios of the three major halons (H-1211 or $CBrClF_2$, H-1301 or $CBrF_3$, and H-2402 or CBr_2F_4) in the troposphere continued to rise (Figure 5.12), because a considerable amount of halon remains stored in fire suppression systems. The growth rates are, however,

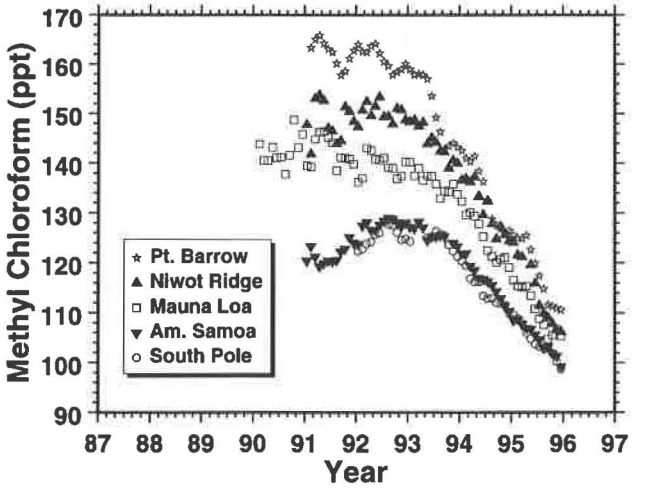

Fig. 5.9. Monthly average CH_3CCl_3 mixing ratios in ppt from the in situ GCs.

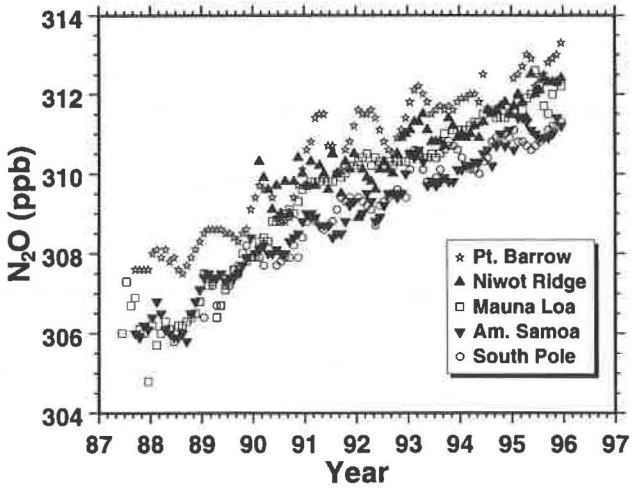

Fig. 5.11. Monthly average N_2O mixing ratios in ppb from the in situ GCs.

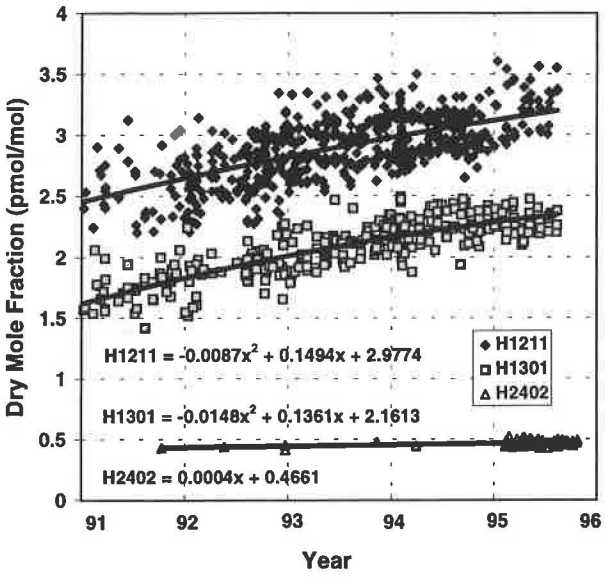

Fig. 5.12. Growth of halons in the atmosphere since 1991. Growth rates are given for January 1, 1994, thus approximating today's increase of stratospheric bromine from halons. Pre-1995 data for H-2402 are from the NOAA archive; all other measurements are from the flask network.

considerably lower now than during the 1970s and 1980s [*Butler et al.*, 1992].

5.1.5. CHLOROFLUOROCARBON ALTERNATIVE MEASUREMENTS PROGRAM

Flask air analysis by GC-MS continued through 1994-1995. Mixing ratios of selected CFCs, HCFCs, HFCs, chlorinated hydrocarbons, brominated hydrocarbons, and halon-1211 were determined from air collected in flasks at the seven remote flask sampling observatories (four CMDL stations and three cooperative flask sampling locations). Toward the end of 1995, flask samples were also collected at three additional sites: KUM, ITN, and HFM.

During this period, analysis methods were developed on a second instrument for precise measurement of halocarbons such as HFCs at mixing ratios of ~0.1 ppt and higher. This was accomplished by using larger volumes of air per injection than in the original GC-MS instrument (up to 1 L of air per injection versus ~0.17 L in *Montzka et al.* [1993]). Detection of halocarbons in this second instrument is also performed with mass spectrometry. Larger flasks (2.4 L) were incorporated into the sampling network in early 1995 to allow for air analysis on this new instrument in addition to other instruments. With these changes and the development of the second GC-MS instrument, measurements of selected HFCs and additional HCFCs became possible in modern air starting in early 1995. Furthermore in 1995, enhanced sensitivity has allowed for the analysis of HFCs, HCFCs, and other halocarbons within archived air samples that were collected at NWR and other locations since 1987.

HCFC-22 ($CHClF_2$) Measurements

The most abundant HCFC, HCFC-22, increased in the global troposphere at a rate of 4.5% yr^{-1} (mean exponential rate estimated from flask samples collected between 1992 and 1996; Table 5.2, Figure 5.13a, and *Montzka et al.*, [1996b]). This rate represents a slower annual increase on a relative basis when compared to growth rates reported for time periods encompassing the 1980s and early 1990s [*Montzka et al.*, 1993; *Zander et al.*, 1994; *Irion et al.*, 1994; *Rinsland et al.*, 1996].

Informal exchange of flask air samples and standards in 1994-1995 with the National Center for Atmospheric Research (NCAR), the University of Bristol, England, and the Scripps Institution of Oceanography has suggested that consistent results (within 5%) can be obtained by chromatographic analysis of air even when different detectors are used (MS and O_2-doped ECD). These results are also reasonably consistent with surface mixing ratios inferred from long-path absorption studies [*Irion et al.*, 1994].

Emission estimates compiled by industry can be used to infer an atmospheric lifetime for HCFC-22. However, uncertainties associated with this exercise limit its usefulness for providing constraints to the global mean burden of the hydroxyl radical. With simple box-model calculations and emission estimates [*AFEAS*, 1995] (without adding additional emission to allow for unreported production), an atmospheric lifetime of 12 ± 2 years is estimated for HCFC-22 from CMDL data. This lifetime is consistent with 11.5 ± 0.7 years, which has been estimated for HCFC-22 based upon a comparison between measurements and model calculations of methyl chloroform [*Prinn et al.*, 1995].

HCFC-141b (CH_3CCl_2F) Measurements

Rapid atmospheric growth continues to be observed throughout both tropospheric hemispheres for HCFC-141b (Table 5.2, Figure 5.13c, *Montzka et al.* [1996b]). Mixing

TABLE 5.2. Annual Mean Growth Rate and Mean Tropospheric Burden (Mixing Ratio) for HCFCs and HFC-134a*, Mid-1994 and Mid-1995

	Mid-1994		Mid-1995	
Compound	Growth Rate, ppt yr^{-1}	Mixing Ratio, ppt	Growth Rate, ppt yr^{-1}	Mixing Ratio, ppt
HCFC-22	5.3	111.1	5.6	116.6
HCFC-142b	1.2	5.6	1.1	6.8
HCFC-141b	1.4	1.9	1.9	3.5
HFC-134a	~0.7†	N.D.‡	1.2	1.6

Global mean growth rates and mixing ratios estimated from polynomial fits to data binned by monthly, bimonthly, odd month, and even month periods, and by station. HCFC-22 growth of 4.5% yr^{-1} is estimated from an exponential fit to global mean data between 1992 and 1996.

*See Figure 5.13. Estimates reported here for HCFC-142b were corrected for an error in Table 1 of *Montzka et al.* [1996b].

†Estimated from mean of two cruises in 1994.

‡Not determined.

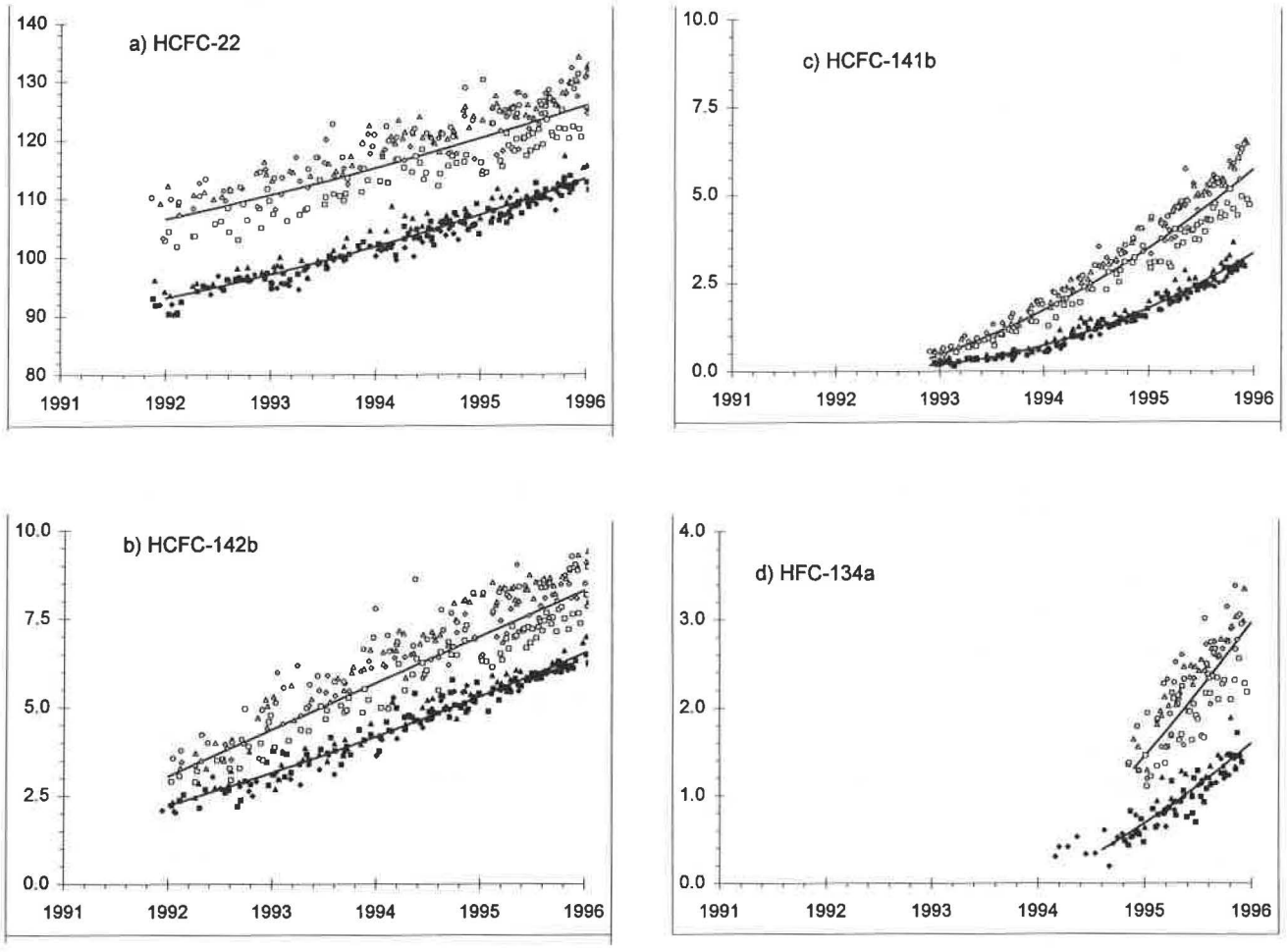

Fig. 5.13. Atmospheric dry mole fractions (ppt) determined since 1992 for the most abundant substitutes for ozone-depleting substances. Each point represents a mean of two simultaneously filled flasks from one of seven stations: ALT, open circles; BRW, open triangles; NWR, open diamonds; MLO, open squares; SMO, filled triangles; CGO, filled squares; SPO, filled diamonds. These data were obtained from the original GC-MS instrument (see text). Solid lines represent fits to hemispheric monthly means.

ratios have increased more than tenfold throughout the global troposphere since the beginning of 1993. Fairly good agreement was reported among different laboratories that have published measurements for this compound [*Montzka et al.*, 1994; *Schauffler et al.*, 1995; *Oram et al.*, 1995].

Preliminary emissions have been estimated recently for HCFC-141b by industry (P. Midgley, Alternative Fluorocarbon Environmental Acceptability Study (AFEAS), personal communication, 1996). At the beginning of 1993, the global tropospheric abundance estimated from the measurements was ~2.0 times greater than the burden estimated from these emissions. By the end of 1994, this ratio had decreased to between 1.3 and 1.4. The exact cause for this discrepancy is currently unknown; however, the difference (but not its time dependence) could be reconciled if emissions are a larger fraction of production than currently assumed. Some of this difference could also be explained by larger vertical gradients within the troposphere than assumed in the simple box-model calculation.

Whereas the atmospheric lifetime of HCFC-141b also influences ambient mixing ratios and affects the magnitude of the difference discussed here, mixing ratios are fairly insensitive to the lifetime chosen for HCFC-141b during the initial phase of use and emission. For example, if we were to consider a lifetime for HFC-141b of 20 years instead of the more accepted value of ~10 years [*WMO*, 1995], the ratio calculated for the end of 1994 would be 1.2-1.3 instead of 1.3-1.4.

Analysis of the CMDL air archive reveals fairly constant mixing ratios of 0.08 - 0.10 ppt for HCFC-141b from 1987 to 1990 (Figure 5.14). After 1990, the abundance increases to ~0.6 ppt in 1993, which is consistent with mixing ratios determined for the northern hemisphere from the flask program at that time [*Montzka et al.*, 1994]. These results are also similar to data reported by *Oram et al.* [1995] where fairly constant mixing ratios of 0.08 ± 0.01 ppt HCFC-141b were found in samples collected at Cape Grim between 1982 and 1991. A dramatic increase was observed at this southern hemispheric site in 1992 and 1993, or 1 to 2 years after that observed at NWR in the CMDL archive.

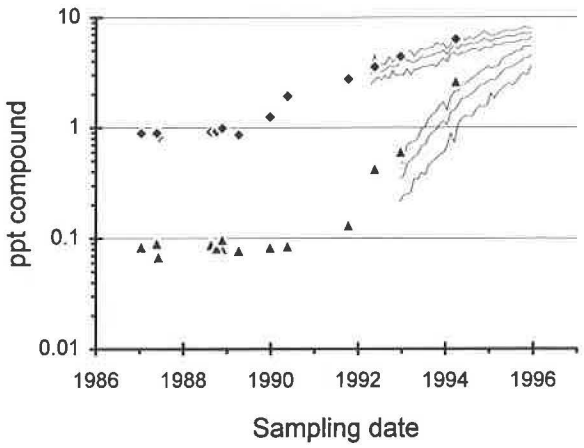

Fig. 5.14. Atmospheric dry mole fractions for HCFC-142b (filled diamonds) and HCFC-141b (filled triangles) in archived air samples as determined on the newer GC-MS instrument. Analyses of archived air were performed in early 1995. With the exception of samples filled in mid-1987, all samples were obtained from NWR or MLO. Samples collected in mid-1987 were obtained shipboard in both hemispheres. Solid lines represent hemispheric (northern always higher than southern) and global monthly means for HCFC-142b and HCFC-141b as determined from the data in Figures 5.13b and 5.13c.

HCFC-142b (CH_3CClF_2) Measurements

Rapid atmospheric growth was also observed for HCFC-142b during 1994-1995 (Table 5.2; Figure 5.13b; *Montzka et al.* [1996b]). Published results from ground-based air samples disagree by ~30%, with CMDL data [*Montzka et al.*, 1994] being higher than mixing ratios reported from the UEA [*Oram et al.*, 1995]. Accurate comparison with a few earlier measurements from NCAR [*Pollock et al.*, 1992; *Schauffler et al.*, 1993] is difficult because these earlier measurements were from air collected above 15 km in northern latitudes. However, from informal exchange of air samples and standards between CMDL and NCAR, and between CMDL and the University of Bristol, mixing ratios determined from these three independent laboratories are expected to span a range of approximately 10% (with CMDL results approximating the mean of the three laboratories: University of Bristol, NCAR, and CMDL).

It is also noted that the mixing ratio reported for HCFC-142b in Table 1 of *Montzka et al.* [1996b] is too high by approximately 6%. The revised growth estimate for 1995 is reduced by a larger percentage (Table 5.2). This error arose in determining the mixing ratio for HCFC-142b in an air sample used for reference in the analysis of flask samples in 1995. This correction does not affect mixing ratios reported or conclusions drawn in *Montzka et al.* [1994]. This error was corrected in public accessible data files (CMDL World Wide Web site) in July 1996.

Emissions estimated by industry from production figures [*AFEAS*, 1995] underestimate the atmospheric burden of HCFC-142b [*Montzka et al.*, 1994; *Oram et al.*, 1995] regardless of which measurements are considered accurate. *Oram et al.* [1995] have suggested that a portion of this discrepancy arises from non-negligible emission of HCFC-142b in the years before 1981, which is the first year for which industry emission estimates are available. Between 1992 and the end of 1995, mixing ratios deduced from these emissions appear to underestimate the atmospheric burden of HCFC-142b by a consistent factor of ~1.9 (CMDL scale).

Analysis of the CMDL NWR air archive in 1995 for HCFC-142b shows mixing ratios of between 0.9 and 1.0 ppt between 1987 and 1989 (Figure 5.14). This is approximately 1.3 times higher than reported by *Oram et al*, [1995] for this period at Cape Grim, and this difference is consistent with calibration differences as discussed above. After 1989, enhanced growth was observed at NWR. The rate of accumulation is believed to have accelerated at Cape Grim approximately 1 year later [*Oram et al.*, 1995].

HFC-134a (CH_2FCF_3) Measurements

Development of techniques for determining mixing ratios of halocarbons present in the atmosphere at ~1 ppt and higher were refined in 1995 on a second GC-MS instrument. This allowed for analysis of air samples for numerous HCFCs, HFCs, and other halocarbons. Archived samples were also analyzed to determine how the abundance of HFC-134a has changed over the past 10 years. Results from these analyses show that the abundance of HFC-134a in the northern hemisphere has risen from ~50 parts per quadrillion (ppq) in 1990 (the limit of detection for this instrument) to ~2.5 ppt in mid-1995 [*Montzka et al.*, 1996a]. Analysis of flask samples filled onboard ship during cruises in 1987, early 1994, and late 1994 show similar atmospheric increases. The abundance of HFC-134a approximately doubled in the time elapsed between the two 1994 cruises in both hemispheres. Cruise flask samples were filled and stored prior to analysis in early 1995 under dramatically different pressures and humidities than the archived samples filled at NWR. The consistency observed between archived samples from NWR and cruise flask samples suggests that the amount of HFC-134a has not been altered significantly during storage by container-related effects and that the measurements are likely representative of atmospheric abundances at the time of sampling.

Routine measurements of HFC-134a in flask samples filled at the CMDL observatories and cooperative sampling locations began in early 1995 (Figure 5.13d; [*Montzka et al.*, 1996a,b]). Mixing ratios for this HFC are increasing rapidly at all sampling locations. Although it is not possible to accurately estimate the growth rate from such a short data record, the increase observed between 1994 and 1996 is consistent with exponential growth at ~100% yr^{-1}.

In simultaneously-filled flasks, mixing ratios determined for HFC-134a were not significantly different. The amount of HFC-134a measured in flasks filled in parallel typically agreed to within 30 ppq and was <100 ppq for 95% of the flask pairs analyzed. Similarly, analysis precision (1 s.d.) for replicate injections of air from flasks collected after 1995 from the ground-based stations was typically <30 ppq (<2%) and was <100 ppq for 95% of the flasks analyzed. This consistency is expected for properly-filled flasks and for molecules not adversely affected by storage in flasks. Flasks received from ground-based stations after February 1, 1995, were analyzed an average of 23 days after sampling.

Preliminary emissions for HFC-134a have recently been estimated by industry (P. Midgley, personal communication, 1996). At the end of 1994, these

emissions overestimate the observed abundance of HFC-134a by only ~0.1 ppt (measured/calculated = ~0.8-0.9).

CMDL Instrument Comparison from Routine Flask Analyses

Beginning in early 1995, large flasks (2.4 L) were filled and analyzed at the stations on both GC-MS instruments. For the compounds shown in Table 5.3, mixing ratios were assigned to air samples based upon independent calibration of reference air with CMDL gravimetric standards. Comparisons of results obtained from these independent instruments can provide further estimates of measurement uncertainty for halocarbons at these low mixing ratios, especially because different analytical conditions are used in the two instruments. The second instrument incorporates a different analytical column (DB-1 versus DB-5), trapping of compounds at different temperatures on a different substrate (a section of alumina PLOT column at −80°C versus a length of uncoated fused silica at −140 to −150°C), and a different valving arrangement. Different mass fragments were monitored during air analysis on the different instruments to determine HCFC-22 mixing ratios (Table 5.3). Because different ions would likely be influenced to different degrees by any coeluting compounds, consistent results obtained with different ions gives additional confidence that these measurements are not affected by such potential chromatographic problems.

Good consistency is observed for measurements of HCFC-22, HCFC-142b, and HFC-134a from the two different instruments. These results suggest that potential problems associated with sample analysis (such as coelution or instrument-specific problems) are not influencing the results that are obtained for these halocarbons on either instrument. A small, consistent offset is apparent for HCFC-141b. The cause of this offset is currently unknown. Variability observed between instruments for measurements of HFC-134a is larger than for other compounds because measured mixing ratios in early 1995 were often near the detection limit on the older GC-MS instrument.

Measurements of Additional Chlorinated Compounds with GC-MS Instrumentation

Mixing ratios for numerous other compounds were determined from flasks during 1994-1995. Data for certain chlorinated hydrocarbons with atmospheric lifetimes of <1 year show dramatic seasonal cycles in both hemispheres (Figure 5.15). Minima for these compounds were observed shortly after midsummer in each hemisphere when loss rates were expected to be greater than at other times of the year.

TABLE 5.3. Results of Individual Flask Air Analysis on Two Different GC-MS Instruments*

	New Instrument to Old Instrument Ratio		Mass to Charge Ratio Ions Monitored	
Compound	Mean	Standard Deviation	New Instrument	Old Instrument
HCFC-141b	0.96	0.04	81	81
HCFC-142b	0.99	0.03	65	65
HCFC-22	1.00	0.03	67	51
HFC-134a	1.00	0.13	83	83

*Comparison based on ~150 flasks analyzed on both instruments in 1995.

Atmospheric Trends for Chlorine and Bromine Contained in Long-Lived Halocarbons

Chlorine and bromine catalyze reactions leading to the depletion of stratospheric ozone. Enhanced use of

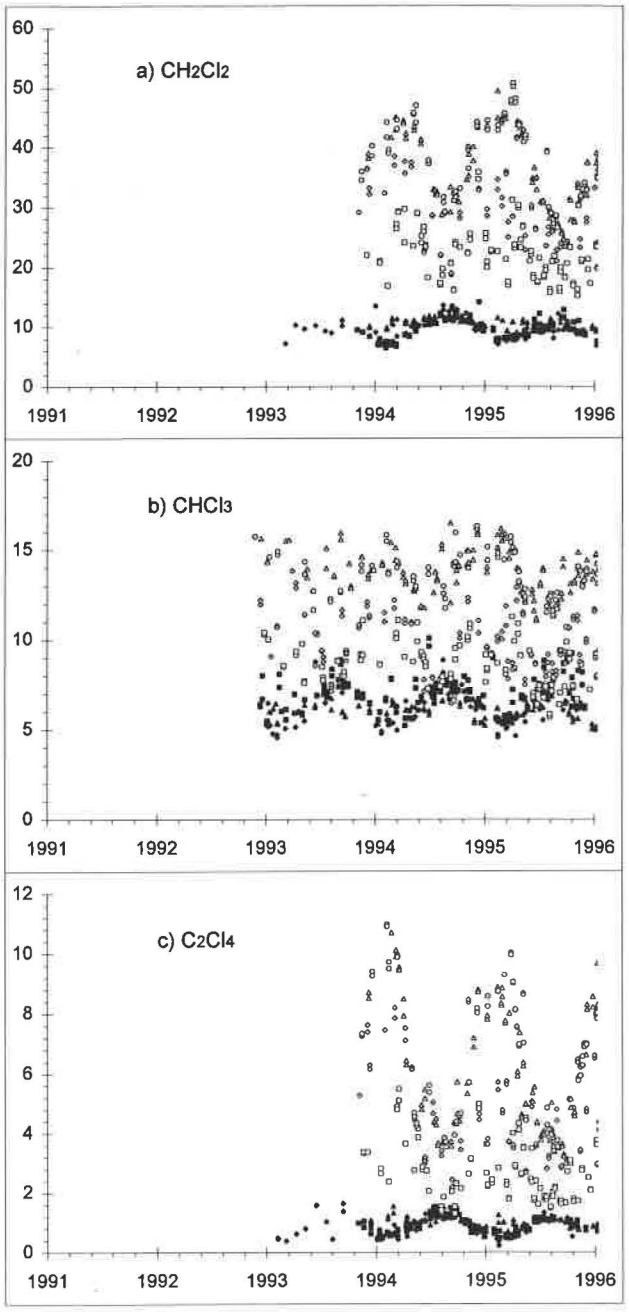

Fig. 5.15. Atmospheric dry mole fractions (ppt) for selected chlorinated compounds. Symbols are identical to those described in Figure 5.13. These data were obtained from flask air analyses on the original GC-MS instrument (see text). Mixing ratios reported are based on a preliminary calibration scale.

chlorine- and bromine-containing compounds by mankind has led to a steady increase in the abundance of chlorine and bromine in the atmosphere in recent time and to the depletion of stratospheric ozone [*WMO,* 1995]. Only bromine and chlorine-containing compounds that are relatively insoluble and have atmospheric lifetimes longer than a year can deliver significant amounts of halogen to the stratosphere. In 1994 the atmospheric abundance of Cl contained in these types of halocarbons was approximately five times greater than the burden estimated in the absence of anthropogenic emissions. Similarly, anthropogenic emissions of bromine-containing compounds have resulted in an atmospheric bromine abundance that is approximately twice that estimated for preindustrial times.

Model studies suggest that the tropospheric abundance of Cl will peak in the mid 1990s at 3.5-4.0 ppb if limits outlined in the most recent Copenhagen amendments to the Montreal Protocol are not exceeded. Not all nations have agreed to the restrictions set forth in the Protocol; in addition, evidence suggests that significant amounts of CFCs are currently produced illegally. Furthermore, developing countries are allowed a 10 year grace period on consumption restrictions under the Montreal Protocol. As a result, much uncertainty has remained regarding the timing and magnitude of peak halogen (Cl and Br) loading of the atmosphere.

In the NOAH Group, global tropospheric distributions and abundances are routinely determined for the most abundant, long-lived anthropogenic halocarbons. Measurements of the halogen burden in the troposphere can supply a reasonable estimate for the stratospheric halogen burden 3 to 5 years in the future [*WMO,* 1995]. Accordingly, the results provide estimates for the burden of ozone-depleting gases in the future stratosphere.

By accounting for the number of Cl atoms contained in the most abundant CFCs, HCFCs, chlorinated solvents, and halon-1211, it is estimated that the tropospheric abundance of Cl contained within these halocarbons peaked in early 1994 and is currently decreasing at a rate of 25 ppt yr^{-1} (Figure 5.16a; Table 5.4) [*Montzka et al.,* 1996b]. The current decrease is a dramatic turnaround from reported increases of 110 ppt yr^{-1} in 1989 and 60 ppt yr^{-1} in 1992 [*WMO,* 1995]. Most of the current decline in tropospheric Cl can be attributed to a decrease in the atmospheric abundance of CH_3CCl_3 (Figure 5.9) which has a relatively short atmospheric lifetime (~5 yr) [*Prinn et al.,* 1995]. The abundance of the major CFCs and chlorinated solvents were all stable or decreasing in 1995 with the exception of CFC-12. The abundance of CFC-12 continued to increase in mid-1995 at a rate of ~6 ppt yr^{-1} or approximately one-third the rate observed in the late 1980s (Figure 5.7 and 5.8). Increases in the abundance of HCFCs (HCFC-22, -142b, and -141b) accounted for growth in tropospheric chlorine of ~11 ppt per year in 1995 [*Montzka et al.,* 1996b]. After accounting for chlorine contributed from CH_3Cl, other chlorinated hydrocarbons (~700 ppt), and less abundant CFCs, it is estimated that the mean global chlorine loading of the troposphere peaked in 1994 at ~3.7 ppb.

Stratospheric ozone is destroyed through reactions of inorganic bromine and chlorine molecules. To estimate how the abundance of stratospheric inorganic halogen will change as a result of the observed trends for halocarbons in the troposphere, stratospheric degradation rates of halocarbons must be considered. Halogen release rates

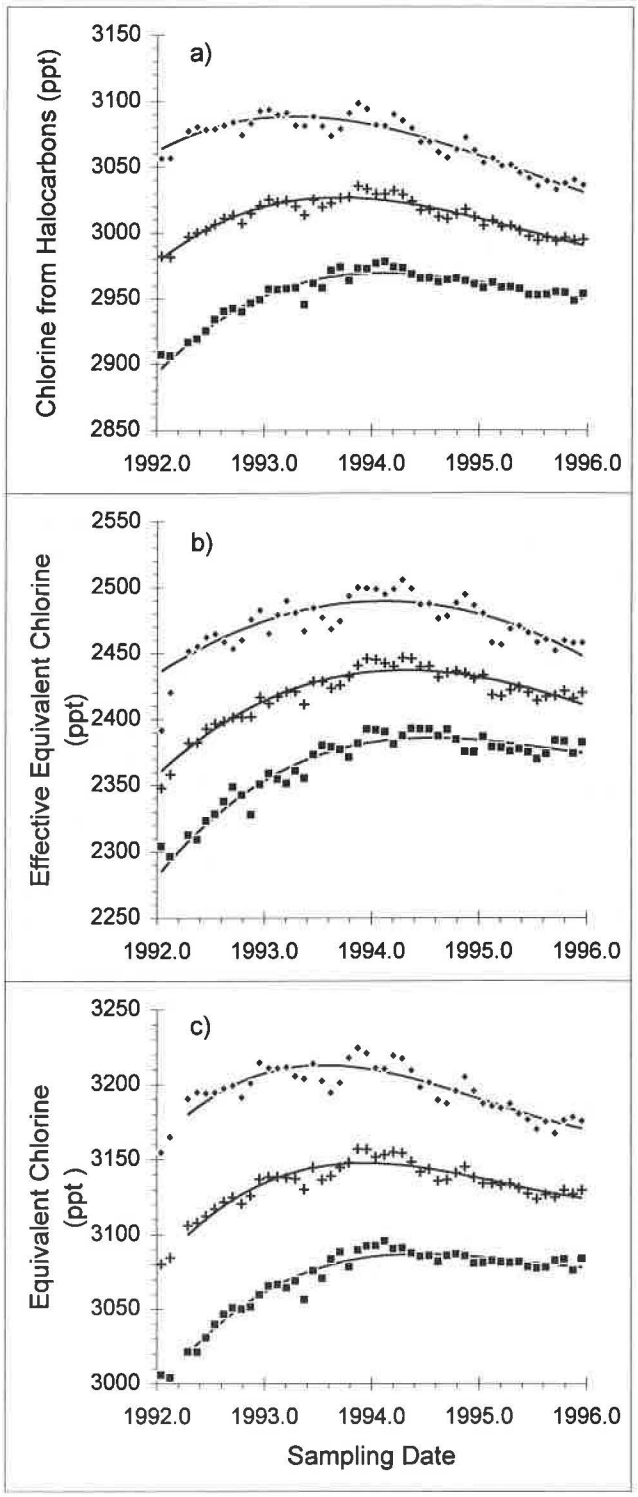

Fig. 5.16. (a) The amount of total chlorine, (b) effective equivalent chlorine (EECl) and (c) equivalent chlorine (ECl) contained within anthropogenic halocarbons: CFC-11, CFC-12, CFC-113, CH_3CCl_3, CCl_4, HCFC-22, HCFC-142b, HCFC-141b, halon-1211, and halon-1301. Data were binned by month and hemisphere (northern hemisphere, filled triangles; southern hemisphere, filled squares; global mean, plus symbols). Solid lines represent fits to monthly means.

TABLE 5.4. Mean Rate of Change Estimated for Mid-1995 From Measured Halocarbons (ppt yr^{-1})*

Compound	Global	NH	SH
Chlorine	-22	-30	-20
EECl	-23	-35	-16
ECl	-15	-22	- 8

*CFC-11, CFC-12, CFC-113, CH_3CCl_3, CCl_4, halon 1211, halon 1301, HCFC-22, HCFC-141b, HCFC-142b.

vary over altitude and latitude in the stratosphere, as does the efficiency for bromine to catalyze the destruction of stratospheric ozone when compared to chlorine (the alpha factor). Whereas bromine is estimated to be about 40 times more efficient than chlorine for destroying stratospheric ozone in the polar vortex [*WMO,* 1995], it may be as much as 100 times more efficient in the lower, midlatitude stratosphere [*Garcia and Solomon*, 1994]. In the following, the future reactive halogen burden is estimated for the lower, midlatitudinal stratosphere (effective equivalent chlorine, EECl) [*Daniel et al.,* 1995] and for the springtime, polar stratosphere (equivalent chlorine, ECl) with halogen release rates and alpha factors appropriate for each region. The abundance of halons increased over this period so that by considering higher estimates for alpha, the decline in EECl or ECl is underestimated.

The current mix and abundance of halocarbons within the troposphere ultimately will release fewer halogen atoms to the lower, midlatitudinal stratosphere than in previous years. The mean global tropospheric burden of halogen that will become inorganic halogen in the stratosphere reached a maximum in early 1994 and was declining in mid-1995 at 21 ± 8 ppt EECl yr^{-1}. (Figure 5.16b; Table 5.4; *Montzka et al.* [1996b]).

The actual rate of change for EECl in mid-1995 may be somewhat lower if the atmospheric abundance of methyl bromide has increased since 1992. However, limits to production outlined in the Copenhagen Amendments and production figures from the major global producers for 1991 and 1992 suggest anthropogenic methyl bromide emissions may have stabilized in the early 1990s. It is unlikely that an increase in methyl bromide over this period would have been large enough to offset the decrease reported here for EECl [*Montzka et al.,* 1996b].

For a mean transport time between the troposphere and lower, midlatitude stratosphere of 3-4 years [*Hall and Plumb*, 1994; *Fahey et al.,* 1995; *Boering et al.,* 1995], maximum levels of inorganic halogen are expected in the lower midlatitudinal stratosphere between 1997 and 1998. Modeling studies suggest that when stratospheric mixing ratios of reactive halogenated compounds begin declining, column-ozone abundance at midlatitudes will begin to recover [*WMO,* 1995]. However, because stratospheric ozone is influenced by other variables such as aerosol loading and temperature [*Solomon et al.,* 1996], the exact timing will also depend on how these variables change over this period.

To estimate the stratospheric abundance of ozone-depleting gases in the springtime polar vortex, equivalent chlorine (ECl) was calculated based upon CMDL tropospheric halocarbon measurements. The current mix and growth rates of these gases in the troposphere will result in lower ECl in the polar stratosphere in the future. In mid-1995 equivalent chlorine was decreasing at 18 ± 7 ppt ECl yr^{-1} (Figure 5.16c; Table 5.4; *Montzka et al.* [1996b]). It is unlikely that an increase in atmospheric methyl bromide in recent time would have been large enough to offset this decrease. Because transport of air from the lower troposphere to the polar stratosphere below ~25 km occurs in 3-5 years [*Prather and Watson*, 1990; *Pollock et al.,* 1992; *WMO,* 1995], or over a slightly longer period than to the lower, midlatitude stratosphere, levels of equivalent chlorine are expected to reach a maximum in the polar stratosphere between 1997-1999 and decline thereafter as long as current growth rates for halons and CFC-12 and the abundance of other CFCs and halocarbons continue to decline.

Although the abundance of reactive halogen in the polar stratosphere above Antarctica will decline when air currently within the troposphere reaches this region, springtime, total-column ozone levels will not increase there immediately. Ozone was nearly completely destroyed in the lower stratosphere above the Antarctic continent in springtime for the past 8 years [*WMO,* 1995]. Total-column ozone abundance within this region is expected to begin recovering only when mixing ratios of reactive halogenated compounds drop below those present in the late 1980s [*Prather and Watson,* 1990; *WMO,* 1995].

5.1.6. GRAVIMETRIC STANDARDS

One of the strengths of NOAH is the ability to generate unique standards for "hot-topic" molecules with ease. Almost all of the NOAH standards are produced by actually weighing the individual components in air or by gravimetry. With maximum dilutions of 1:20,000 and accuracy's of better than 0.2%, two or four dilutions are sometimes required to produce standards at the ppt level. Not only does NOAH produce standards for internal use, but some of the clients have included other international and national research institutions. Some of this work over the past 2 years is summarized below.

Aluminum compressed gas cylinders are now being used with brass and stainless steel valves that have all-metal valve stems and seats. Materials such as KEL-F have a high absorption/desorption potential for gases such as 1,1,2-trichloro-1,2,2-trifluoroethane (CFC-113).

Five compressed gas cylinders containing pure reagent gases were analyzed for impurities using a CEC-103 mass spectrometer located at the National Institute of Standards and Technology (NIST) in Gaithersburg, Maryland. The results of the analyses indicated that the measured purity levels of the pure methane (CH_4), carbon monoxide (CO), carbon dioxide (CO_2), hydrogen (H_2), and nitrous oxide (N_2O) gases are consistent with the stated purity as specified by the gas supplier. These pure mixtures are being used to prepare gravimetric standards for CCG (CH_4, CO, CO_2, and H_2) and for NOAH (N_2O).

A total of 26 gravimetrically prepared CH_4 in air standards now exist for use by CCG. The nominal mixing ratios of the gas mixtures range from 32 ppb to 20 ppm. The standards are currently being studied for stability.

A suite of gravimetrically prepared sulfur hexafluoride (SF_6) in air standards were prepared for the first time this year. The standards were prepared with nominal mixing ratios ranging from 3 ppt to 110 ppt.

A suite of hydrogen (H_2) in air standards were also gravimetrically prepared for the first time this year. The mixing ratios of these standards range from approximately 450 ppb to 600 ppb.

HFC-134a in air standards were prepared in 1995 and were intercompared with existing HFC-134a standards prepared several years ago. The results confirm that the gas is stable over many years.

Several nine-component standards containing various methyl halide compounds were gravimetrically prepared primarily for the ocean and flask programs. The standards contain methyl bromide (CH_3Br), methyl chloride (CH_3Cl), methyl iodide (CH_3I), dibromomethane (CH_2Br_2), tribromomethane ($CHBr_3$), chlorodibromomethane ($CHBr_2Cl$), bromochloromethane (CH_2BrCl), chloroiodomethane (CH_2ICl), and diiodomethane (CH_2I_2). Nine two-component mixtures were initially prepared with mixing ratios at the ppb level. The pure liquids were handled under darkroom conditions with the use of a black-light source, because compounds with iodine are photochemically active and decompose quickly in sunlight and artificial light.

Existing CH_3CCl_3 and CCl_4 primary standards at the ppb level were compared to standards recently prepared to determine the stability of these gases over a number of years and to resolve a difference in sensitivity between several suites of ppt level standards that were prepared from the ppb standards. The mixing ratios range from 120 ppb to 760 ppb for CH_3CCl_3 and from 190 ppb to 950 ppb for CCl_4. The gases were analyzed using GC with a FID. The results of the analyses indicate that eight of nine CH_3CCl_3 standards and nine of nine CCl_4 standards are consistent to within ±2%.

5.2. Aircraft GC Project: ASHOE/MAESA Mission

5.2.1. Overview

A new four-channel GC, Airborne Chromatograph for Trace Atmospheric Species (ACATS-IV), was deployed for the first time in 1994 as part of the year-long Airborne Southern Hemisphere Ozone Experiment/Measurements for Assessing the Effects of Stratospheric Aircraft (ASHOE/MAESA) mission. ACATS-IV flew successfully on 24 flights spanning latitudes from 70°S to 60°N during four seasons. During ASHOE/MAESA, ACATS-IV was configured to measure ten different molecules. In addition to CFC-11, CFC-113, and CH_4 (compounds measured previously with a two-channel version of the instrument) ACATS-IV measured CH_3CCl_3, CCl_4, CFC-12, H-1211, N_2O, SF_6, and H_2. ACATS-IV provides an important set of tracer measurements for several different aspects of atmospheric research: (a) Dynamic and chemical models can be constrained by the wide range of these tracer's lifetimes (4.5-3200 years). (b) Halogens play an important role in stratospheric ozone destruction and ACATS-IV provides in situ stratospheric measurements of 80% of the chlorine containing species and the bromine containing compound, H-1211 which contains about 20% of the total organic tropospheric bromine. (c) Apart from tropical transport of water from the troposphere to the stratosphere, CH_4 oxidation is the largest source of stratospheric water, which has a large global warming potential. Simultaneous CH_4, hydrogen, and water measurements completely constrain the stratospheric hydrogen budget. (d) The age of stratospheric air is an important input to atmospheric models. SF_6 is a purely anthropogenic compound with no known tropospheric sinks, a stratospheric lifetime of 3200 years, and an approximately linear tropospheric growth rate that makes it an excellent indicator of the age of stratospheric air.

A complete instrument description can be found in a recent publication by *Elkins et al.* [1996]. The GC has been optimized for low ppt work and frequent sampling of 3-6 minutes by using an appropriate choice of separation columns, very sensitive ECDs, and 12-port gas sampling valves that permit heart-cutting the chromatogram (Figure 5.17). The measured tracers have a wide range of lifetimes that can be used to estimate a tropical-midlatitude exchange in the stratosphere as demonstrated in *Volk et al.* [1996]. The H-1211, SF_6, CFC-11, and CFC-12 measurements from ASHOE/MAESA have also been incorporated into a calculation that indicates the oldest stratospheric air measured by ACATS-IV has 17 ± 3 ppt of bromine and that all of the bromine resides in inorganic form.

5.2.2. Transport in the Lower Stratosphere

ACATS-IV observations in the lower tropical and midlatitude stratosphere during ASHOE/MAESA provide new information about mass exchange between the tropics and midlatitudes. Because of the profound impact of transport on the distribution of long-lived stratospheric constituents, the magnitude of such exchange is critical for prediction of ozone depletion by human activities. The sparse set of previous tropical in situ tracer data [*Goldan et al.*, 1980; *Murphy et al.*, 1993] and satellite observations of tracer and aerosol distributions [*Trepte and Hitchman*, 1992; *Randel et al.*, 1993; *Mote et al.*, 1996] have provided evidence for a subtropical "barrier" to horizontal exchange. These observations led to the suggestion that the stratosphere might be closer to a "tropical pipe" model [*Plumb*, 1996], in which tropical air ascends in isolation from midlatitude influence, than a "global diffuser" model [*Plumb and Ko*, 1992]. For the first time the ASHOE/MAESA campaign provided extensive tropical measurements of many tracers with local lifetimes ranging from less than 1 to 100 years. These data provide a powerful tool for quantifying the amount of transport across the subtropical barrier. A simple tropical tracer model was used to analyze ACATS data for CFC-11, CFC-12, CFC-113, CCl_4, CH_3CCl_3, halon-1211, and CH_4 along with measurements of N_2O, NO_y, and O_3 from three other instruments aboard the ER-2 [*Podolske and Loewenstein*, 1993; *Fahey et al.*, 1989; *Proffitt and McLaughlin*, 1983]. The observations during ASHOE/MAESA span latitudes from 60°N to 70°S and altitudes up to 21 km. The model considers the vertical evolution of a tropical tracer, including loss and production resulting from local photochemistry and entrainment of midlatitude air (due to isentropic mixing):

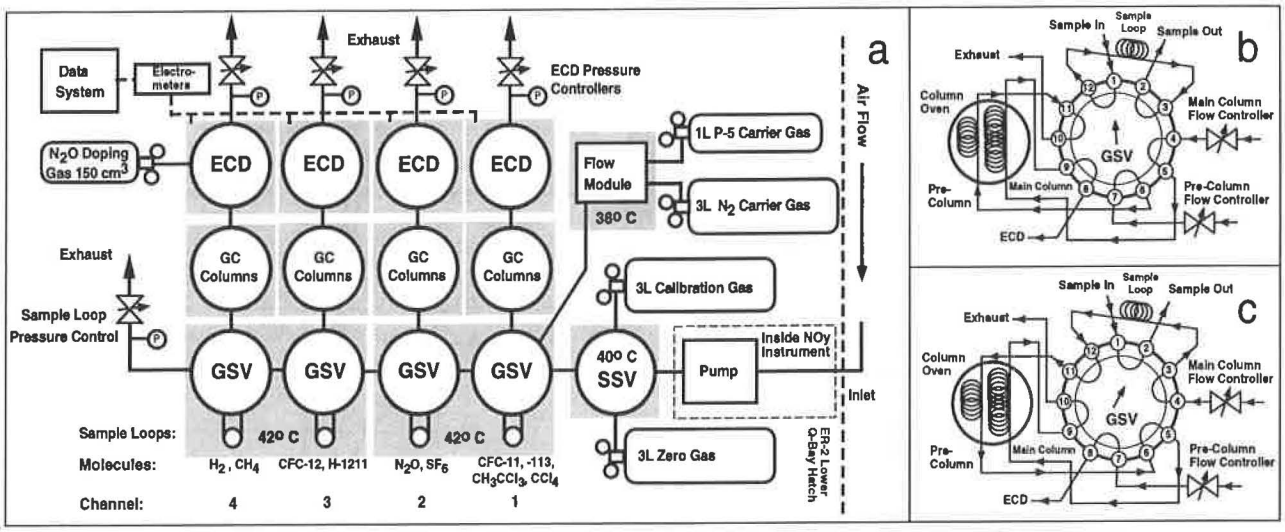

Fig 5.17. (a) Schematic of the ACATS-IV instrument showing pressure transducers (P), electron capture detectors (ECD), gas sampling valves (GSV), and the stream selection valve (SSV). Shaded areas are temperature-controlled zones where the temperatures for the GSV, SSV, and flow module are indicated. ECD and sample loop pressure controllers use a valve (MKS Instruments, Inc., Andover, Massachusetts) servo-controlled to a pressure gauge (Micro Gage, Inc., El Monte, California). The GC inlets for the calibration, carrier gases, and air sample have 10 μm screens to remove particles. (b) The first position of the 12-port GSV permits loading the sample loop, backflushing of the pre-column, and detection of the peaks of interest from the previous sample injection. (c) Turning the rotor of the 12-port GSV allows injection of the sample onto the columns and diversion of the column exhaust away from the ECD.

$$\frac{\partial \chi}{\partial \theta} Q = P - \frac{\chi}{\tau} - \gamma\chi - \frac{\chi - \chi_{mid}}{\tau_{in}} \qquad (1)$$

where χ and χ_{mid} are the mean tropical and midlatitude mixing ratios; θ is potential temperature used as vertical coordinate; $Q = d\theta/d\tau$ is the net diabatic heating rate, equivalent to vertical ascent rate; P is the photochemical production rate; τ is the lifetime for photochemical loss; γ is the long-term growth rate; and τ_{in} is a time scale for import of midlatitude air, the quantity to be determined by this analysis. Tropical ascent rates (Q) were obtained from published calculations [*Rosenlof*, 1995; *Eluszkiewicz et al.*, 1996]; chemical production and sinks for the species considered were calculated with a radiative transfer model [*Minschwaner et al.*, 1993] and a photochemical model [*Salawitch et al.*, 1994]; and long-term growth rates (γ) were derived from CMDL network data. Midlatitude mixing ratios were constrained from observations between 35° and 55° in both hemispheres. Tropical air was identified as the region equatorward of the sharp meridional gradient in the NO_y/O_3 ratio observed in the subtropics [*Murphy et al.*, 1993].

A qualitative impression of the isolation of the tropical ascent region can be gained by comparison of vertical profiles of tracer mixing ratios observed in the tropics to profiles calculated assuming unmixed ascent (unmixed profiles), i.e., solutions to Eq. (1) with $\tau_{in} = \infty$ (Figure 5.18). Observed profiles of the longer-lived species, N_2O and CFC-12, and also of CH_4 and NO_y (not shown) deviate noticeably from unmixed profiles, indicating mixing with photochemically aged midlatitude air. However, for CFC-113, CFC-11, and the shorter-lived species CH_3CCl_3, CCl_4, and halon-1211 (not shown), observed profiles fall within the uncertainty range of values calculated for unmixed ascent because their vertical profiles are controlled primarily by photochemical loss that dominates loss by mixing for these shorter-lived species.

Quantitative derivation of the rates of transport between the tropics and midlatitudes is best achieved by analyzing correlation diagrams of two species with disparate lifetimes [*Volk et al.*, 1996]. Differences in the slopes of correlations observed at midlatitudes and in the tropics provide a direct measure of exchange between the two regions if horizontal mixing is fast compared to photochemistry for one of the two species (but not both). As an example, for a given mixing ratio of N_2O, the shorter-lived species show lower abundances in the tropics than at midlatitudes because their loss processes are larger near ~20 km (Figure 5.19), whereas N_2O is not destroyed until the air reaches higher altitudes. Because the abundance of N_2O in the tropics is sensitive to isentropic mixing, however (Figure 5.18), the tropical correlations do not match the correlations calculated assuming unmixed ascent.

In order to derive the entrainment time (τ_{in}) from the correlation diagrams in Figure 5.19, we consider Eq. (1) for the tropical mixing ratios of two tracers X and Y:

$$\frac{\partial Y}{\partial X} = \frac{P_y - (\tau_y^{-1} + \gamma_y)Y - \tau_{in}^{-1}(Y - Y_{mid})}{P_x - (\tau_x^{-1} + \gamma_x)X - \tau_{in}^{-1}(X - X_{mid})} \qquad (2)$$

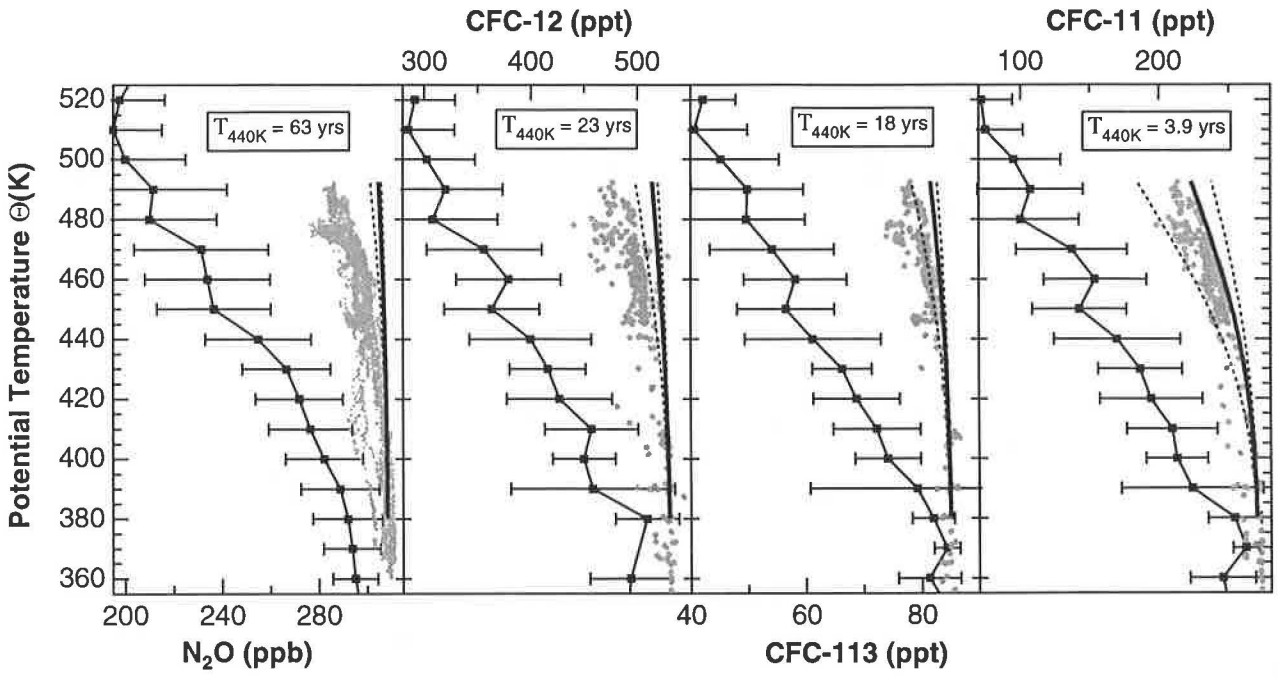

Fig. 5.18. Vertical profiles of mixing ratios of several long-lived trace species in the tropics (light filled circles) and at midlatitudes (dark filled squares) [*Volk et al.*, 1996]. For the midlatitudes the data was binned into 10K increments of potential temperature (θ); the profiles shown represent the bin averages and the error bars represent the standard deviation within each bin. Calculated tropical profiles are shown for unmixed ascent ($\tau_{in} = \infty$) (—) from θ = 380K (the mean tropical tropopause height) along with an uncertainty range induced by a 50% uncertainty in Q (---). Also indicated is the "effective lifetime" T ($=1/(\tau^{-1}+\gamma)$) at θ = 440 K (~19 km altitude) for each of the species.

Eq. (2), constrained by the mixing ratios for midlatitudes from observations and computed photochemical sources and sinks, is solved to calculate the tropical correlation Y(X) of two species; the entrainment time τ_{in} is treated as a free (altitude-independent) parameter. For each pair of tracers displayed in Figure 5.18, the value of τ_{in} is determined giving best agreement between the calculated tropical correlations (Figure 5.19) and the observations. The same procedure was also applied to correlation diagrams of the longer-lived species, CH_4, N_2O, CFC-12, CFC-113, and NO_y, versus O_3, which is shorter-lived (with a photochemical production time of only ~3.5 months at 19 km). Analysis of each correlation diagram yielded a mean for τ_{in} of 13.5 months, with an uncertainty of ~20%. This seasonally and vertically-averaged entrainment time is longer than the time scale for isentropic mixing at midlatitudes of less than 3 months [*Boering et al.*, 1995], confirming that mixing into the tropics is slow compared to mixing within midlatitudes. Because of the variability of the tropical correlations and the limited seasonal coverage, the data do not provide information on the dependence of τ_{in} with height.

Entrainment of air into the tropics is not necessarily balanced by poleward detrainment from the tropics. In the annual mean, the net mass flux out of the tropics (detrainment minus entrainment) must be balanced by the mean mass divergence within the tropics (that can be determined from the mean ascent rate):

$$\frac{\rho}{\tau_{out}} - \frac{\rho}{\tau_{in}} = -\frac{\partial}{\partial z}(\rho w) \qquad (3)$$

where τ_{out} is a time scale for export of air whose inverse is the detrainment rate; ρ is the air density; z is altitude; and w is the mean vertical velocity. Detrainment rates computed from Eq. (3) for the estimate of τ_{in} (13.5 months) and ascent velocities averaged over 24 months, show that over much of the altitude range considered, more air is exported from the tropics than is imported (Figure 5.20a). The corresponding detrainment time (τ_{out}) of less than ~6 months below 19 km and the morphology of decreasing detrainment with altitude is consistent with observations of the propagation of the seasonal cycles of CO_2 and H_2O from the tropics to midlatitudes [*Boering et al.*, 1995; *McCormick et al.*, 1993] and with studies of aerosol dispersal from the tropics [*Trepte and Hitchman*, 1992].

As shown in Figure 5.20b, for an entrainment time of 13.5 months, ~45% of air of extratropical origin accumulates in a tropical air parcel during its ~8 month ascent from the tropopause to 21 km. The large uncertainty range in this result (Figure 5.20b) results from the uncertainty of the ascent velocity. This substantial entrainment of midlatitude air into the tropical ascent region of the lower stratosphere implies that a significant fraction of NO_x (=NO + NO_2) and other effluents emitted

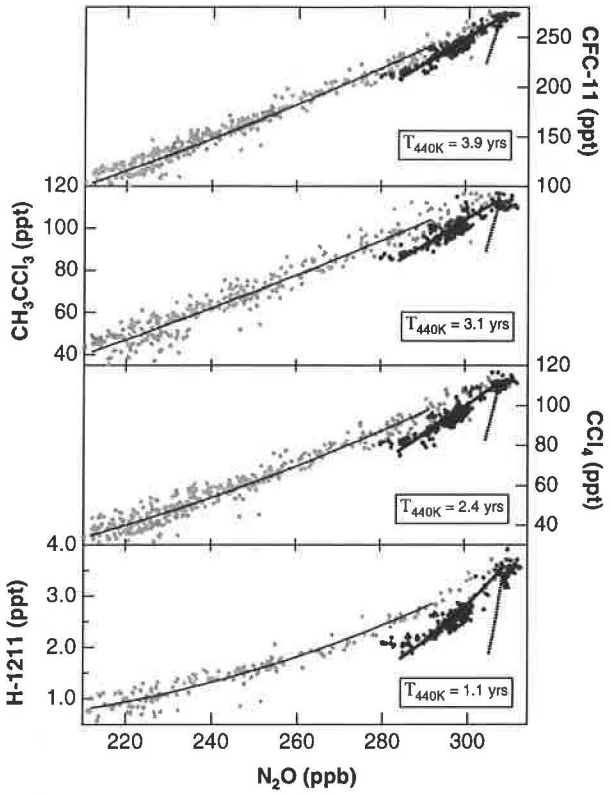

Fig 5.19. Correlations of mixing ratios for the shorter-lived species versus N_2O in the tropics (dark filled circles) and at midlatitudes (light filled circles) [Volk *et al.*, 1996]. Mean midlatitude correlations used in the model (long dash) were obtained from quadratic fits to the correlations. Calculated tropical correlations are shown for the unmixed case (τ_{in}= ∞) (short dash) and for a constant entrainment time τ_{in} that yielded the best agreement (in a least-squares sense) with the observed tropical correlations (long dash). Also indicated is the "effective lifetime" T (= $1/(\tau^{-1}+g)$) at θ = 440 K for each of the species.

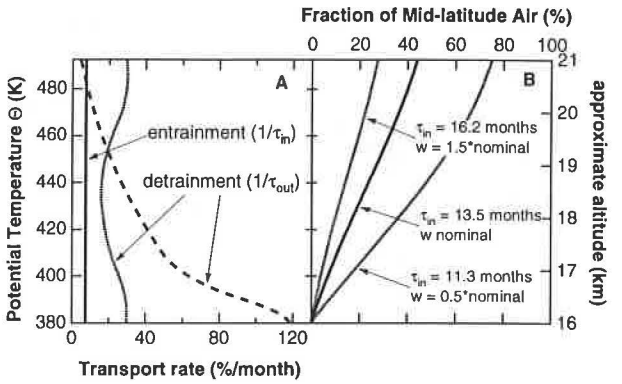

Fig 5.20. (a) Entrainment rate into and detrainment rates out of the tropics versus potential temperature, expressed as % of air within a tropical air volume (at a fixed altitude) entrained/detrained per month [*Volk et al.*, 1996]. Results are for τ_{in} =13.5 months and ascent rates from *Rosenlof* [1995] (short dash) and *Eluszkiewicz et al.* [1996] (dotted). The disagreement between the detrainment rates based on these two studies reflects differences in the vertical profiles of the ascent rates. (b) Fraction of midlatitude air within the tropics versus potential temperature for nominal (long dash) and extreme (dotted) values of τ_{in} and ascent rates w from *Rosenlof* [1995] as indicated.

from supersonic aircraft at midlatitudes between 16 and 23 km will likely reach the middle and upper stratosphere where enhancements in NO_x are expected to lead to reductions in ozone [*Stolarski et al.*, 1996].

While estimating the effects of human activity on ozone remains a task for multi-dimensional models of atmospheric transport and chemistry, the determination of the rates of transport and the fraction of midlatitude air within the tropical ascent region constitutes important tests for the accuracy of such models. Most current 2-D models do not reproduce steep meridional tracer gradients in the subtropics such as observed in the NO_y/O_3 ratio [*Murphy et al.*, 1993], suggesting they generally overestimate the magnitude of mixing between the tropics and midlatitudes. Tests with a particular two-dimensional model show that greater reductions of midlatitude ozone are calculated, improving agreement with observed trends, if mixing parameters are modified to simulate restricted exchange across the tropics [M.K.M. Ko, private communication, 1996]. Realistic representation of dynamical coupling between the tropical source and midlatitude sink regions of ozone may thus hold the key to understanding and reliably predicting the response of the stratospheric ozone layer to a variety of anthropogenic as well as natural perturbations.

5.2.3. Bromine Budget

Concern over bromine's contributions to stratospheric polar ozone loss [*McElroy et al.*, 1986] and potential for midlatitude ozone destruction [*Yung et al.*, 1980] has resulted in an international regulation of halons and methyl bromide. These bromine-containing compounds occur at much lower stratospheric mixing ratios than chlorine-containing compounds, but bromine is 40-100 times more efficient than chlorine at destroying ozone in the lower stratosphere [*WMO*, 1995]. In an effort to improve the understanding of brominated compounds in the stratosphere, the first real-time, in situ stratospheric measurements of the purely anthropogenic compound, $CBrClF_2$ (H-1211) [*Elkins et al.*, 1996] were obtained. Measurements of H-1211 and nine additional tracers were obtained in 1994 at latitudes ranging from 70°S to 60°N and to altitudes of 20 km as part of the ASHOE/MAESA mission. The complete H-1211 data set for ASHOE/MAESA is shown in Figure 5.21. These measurements were incorporated into a calculation of the total 1994 stratospheric bromine burden. The lower stratosphere was calculated to contain 17 ± 3 ppt of bromine in 1994 and that essentially all of the organic bromine had been converted to inorganic forms.

The total stratospheric bromine burden was calculated by summing the bromine content in the tropospheric organic bromine species with lifetimes long enough to allow their transport to the stratosphere. This approach assumed that the only source of stratospheric bromine is at the earth's surface. The organic bromine species included in the model are CH_3Br, H-1211, H-1301, CH_2Br_2, H-2402, and CH_2BrCl with November 1994 mixing ratios of 10.1, 3.3, 2.3, 1.1, 0.47, and 0.14 ppt respectively. The CMDL background site monitoring program provided a historical record of H-1211, H-1301, H-2402, and CH_2Br_2. The CH_3Br data were collected on transects of the Atlantic and Pacific Oceans in 1994 by CMDL researchers

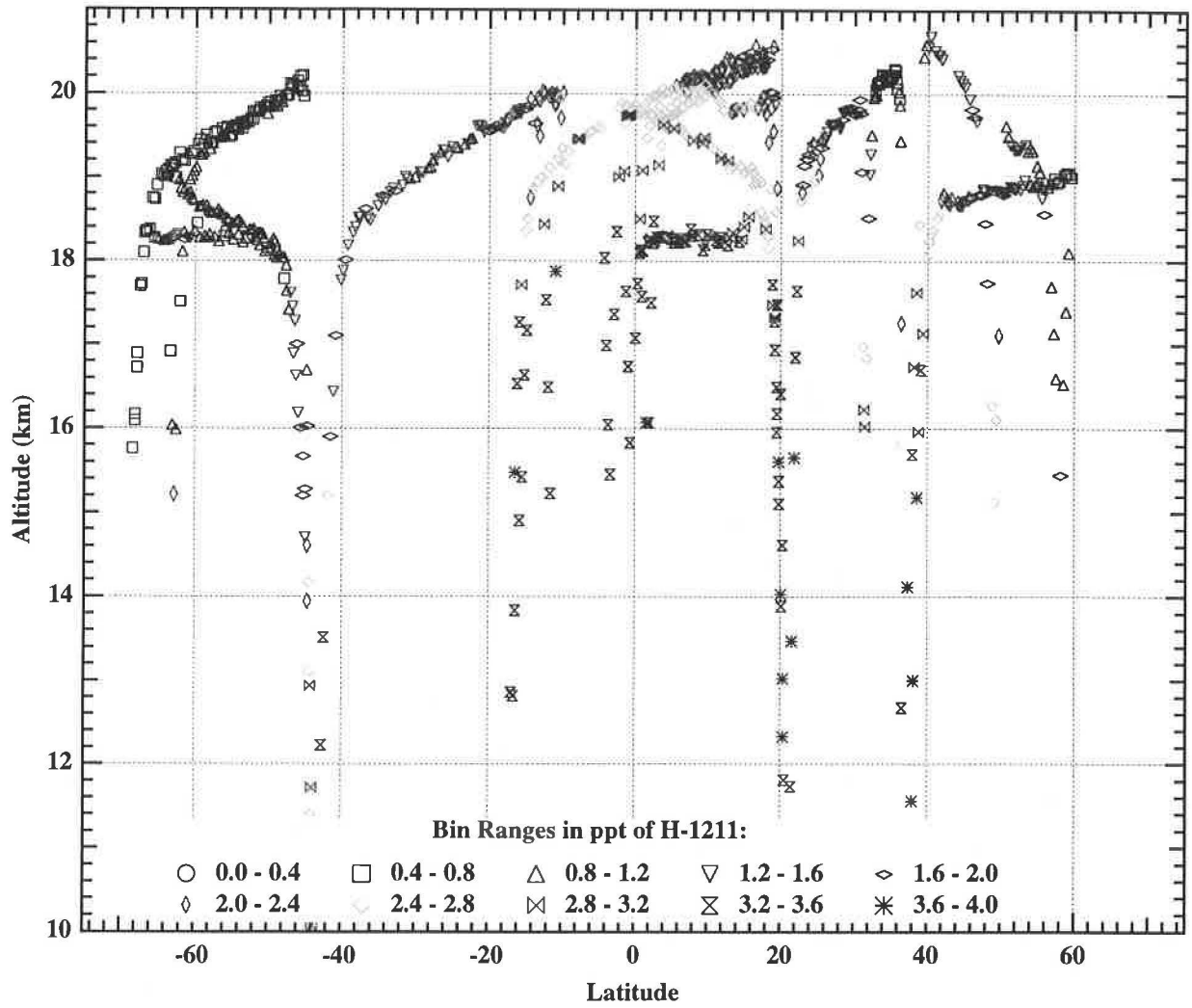

Fig. 5.21. Latitudinal profile of halon-1211 as a function of pressure (mb). ACATS-IV measurements of halon-1211 in ppt during ASHOE/MAESA.

[*Lobert et al.*, 1995]. The CH_2BrCl data are from Whole Air Sampler (WAS) measurements taken by researchers at NCAR in early 1995. Taking the weighted sum of the mixing ratios of these species yields the following equation for the total bromine contained in these species as a function of time.

$$\begin{aligned} &\text{Tropospheric } [CBr_y](t) = \\ &[CH_3Br] + [\text{H-1211}](t) + \\ &[\text{H-1301}](t) + 2[CH_2Br_2] + \\ &2[\text{H-2402}](t) + [CH_2BrCl] = \\ &8.64 + (0.2863t) + (-0.0235\ t^2) \end{aligned} \quad (4)$$

where t is time in years measured from 1994. The tropospheric burden of these species provides an upper limit on the concurrent stratospheric bromine burden. ACATS-IV ASHOE/MAESA measurements of the sulfur hexafluoride (SF_6) mixing ratios are used to determine the age of the stratospheric air and thus, the total bromine present in the air being sampled.

Photolysis of the organic bromine species produces inorganic bromine species with the majority of the inorganic bromine in reactive forms. The partitioning of stratospheric bromine was calculated using the equation

$$\text{Total Bromine} = \text{Organic Bromine} + \text{Inorganic Bromine} \quad (5)$$

where Total Br is determined as outlined previously. The only organic bromine species that ACATS-IV measured is H-1211, but from whole air sampler measurements from NCAR (Schauffler, private communication, 1996) and the University of California, Irvine (Blake, private communication, 1996), correlations were compiled of the unmeasured species with measured CFCs. These correlations are shown in Figure 5.22. These correlations permit an estimate of total organic bromine (Figure 5.23).

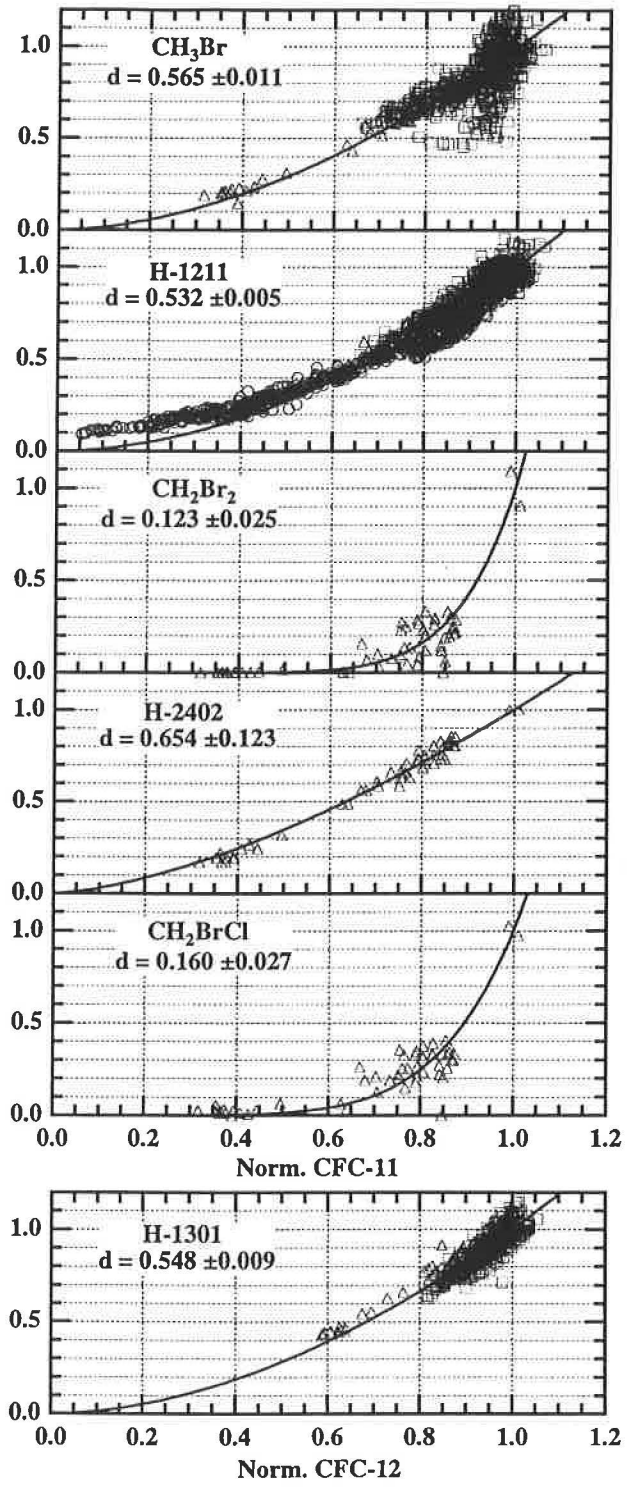

Fig. 5.22. Correlations of bromine-containing species with CFC-11. The longest-lived species, H-1301, is correlated with CFC-12. Each data set was normalized individually and then the complete data set for each species was fit with a function of the form $[X_n] = [CFC_n]^{(1/d)}$, where the subscript, n, represents a normalized quantity. The longest lived species, H-1301, is correlated with CFC-12. ACATS-IV data are shown by circles. NCAR data are denoted by triangles and UC-Irvine data are shown by squares.

The oldest air sampled by ACATS-IV during ASHOE/MAESA indicated that all of the stratospheric bromine was in inorganic forms.

5.3. LACE

A new project titled Lightweight Airborne Chromatograph Experiment (LACE) is a 2-channel GC designed to measure CFC-11, CFC-113, and SF_6. It was built to fly on a balloon and take data from altitudes up to 32 km. This will complement the lower altitude NASA ER-2 data, help solidify understanding of atmospheric dynamics, and provide a comparison for midlatitude and tropics chemistry. NOAH scientists used the ACATS-IV instrument as a starting point; however, several key differences have been introduced. The balloon's fast decent of 2.5 m s^{-1} imposes a faster data sample rate of 1 minute to acquire reasonable coverage of data every 150 m. Sample rates for the ACATS-IV instrument are currently 3 and 6 minutes with the exception of one recent flight where the new 1-minute chromatography (Figure 5.24) was successfully flown. Because of the higher altitude, clean air samples must be loaded from an ambient pressure of only 10 mb compared to an ambient pressure of 50 mb or higher for the ACATS instrument. Finally, in contrast to the ER-2's Q-bay, which is pressurized to a minimum of 300 mb and houses the ACATS instrument, the balloon platform required a self-pressurized, lighter-weight instrument that uses less power.

Problems solved in building this GC for a balloon platform were similar to those that will occur when placing an instrument in a remotely piloted aircraft (RPA) like Perseus. When an operational RPA becomes available, LACE can be easily modified for flight on this type of platform.

5.4. Ocean Project: BLAST Cruises

In 1994 the NOAH Group participated in two research cruises for the Bromine Latitudinal Air/Sea Transect (BLAST) project. The first cruise extended through the East Pacific between Seattle, Washington, and Punta Arenas, Chile, from January 26 to February 17, 1994; the second cruise was conducted between October 18 and November 21, 1994, heading through the Atlantic Ocean from Bremerhaven, Germany, to Punta Arenas, Chile (Figure 5.25). The main objective of these cruises was to gather data to ascertain the presence or absence of a potential oceanic source for methyl bromide (CH_3Br). Methyl bromide contributes about 50% to tropospheric organic bromine and, hence, has received considerable attention, particularly because its budget is currently not well understood [*Butler*, 1995, 1996; *Butler and Rodriguez*, 1996]. Frequently collected CH_3Br data from the two expeditions constitute the largest data set for oceanic CH_3Br to date and the first solid estimate of oceanic emission, production, and chemical degradation of the compound. It is concluded from these studies that the ocean is not a net source of CH_3Br but rather a net sink [*Lobert et al.*, 1995, 1996; *Butler et al.*, 1995]. Although CH_3Br is both produced and consumed everywhere in the surface ocean [*Butler*, 1994], the rate of consumption exceeds that of production in most waters sampled. Exceptions were coastal and coastally-influenced waters,

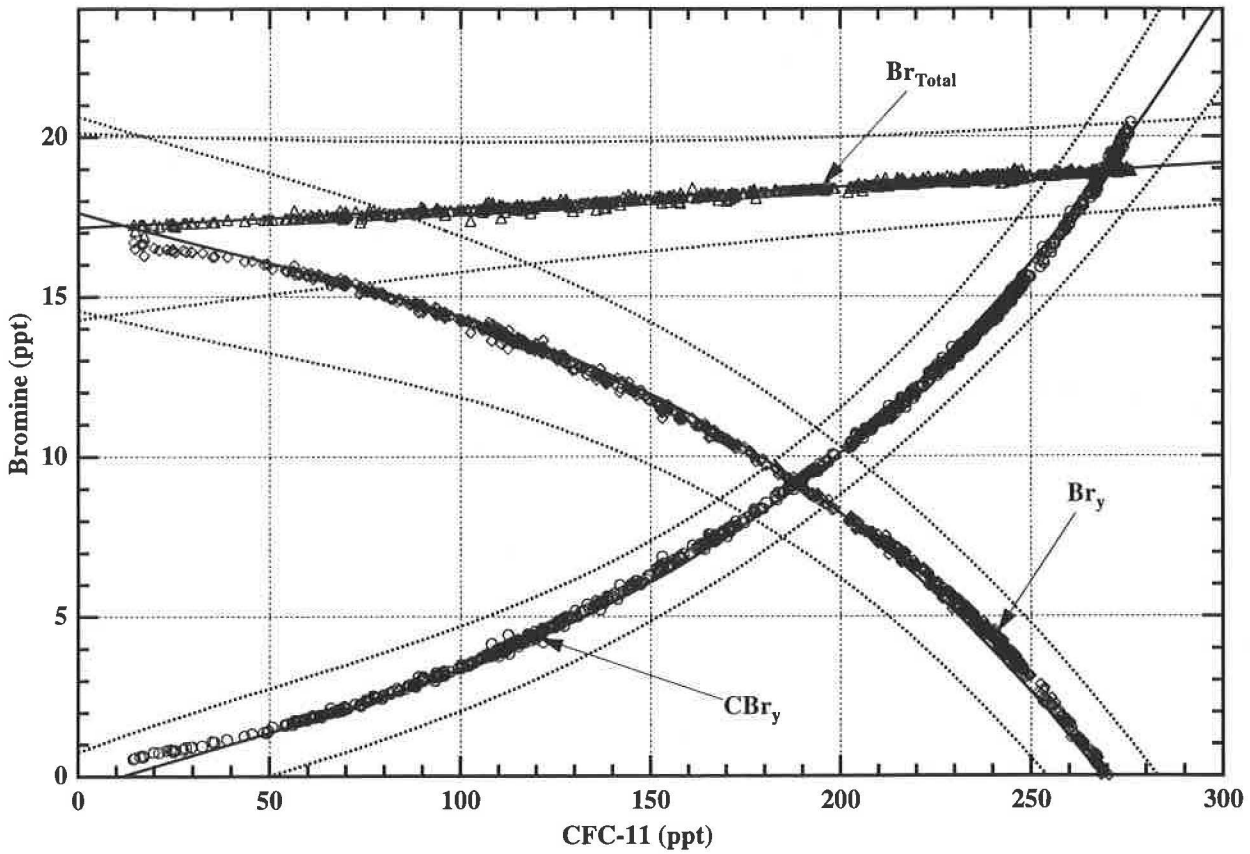

Fig. 5.23. Calculated results for the total stratospheric bromine, Br_{total}, (open triangles), and its partitioning into total organic CBr_y (open circles), and inorganic, Br_y (open diamonds), components. The dashed lines represent standard deviation windows.

which were typically supersaturated, and areas of open ocean upwelling, where CH_3Br saturation anomalies were close to zero. About 80% of the oceans are undersaturated in CH_3Br, representing a net annual sink of 8-22 Gg yr^{-1}.

CH_3Br data from the second cruise further supported NOAH conclusions from the first expedition. The latter results give greater strength to the global extrapolations of the first data set. Data from the two cruises are summarized in Table 5.5 and Figure 5.26.

The best estimate of the partial lifetime of atmospheric CH_3Br with respect to oceanic losses is 2.7 (2.4-6.5) years. This range was derived from a 40-year, global data set of sea surface temperatures and wind speeds [*Yvon and Butler*, 1996] (Figure 5.27). Data from the two expeditions suggested a shorter lifetime of CH_3Br of about 2.4 years. The difference between the two estimates is due to higher than average wind speeds encountered during the cruises. The estimated atmospheric lifetime, based upon combined atmospheric, soil, and oceanic losses, is now 0.8 years compared to earlier estimates of 1.8-2.1 years when the ocean was considered an insignificant sink, the soil sink [*Shorter et al.*, 1995] was unknown, and tropospheric OH concentrations were underestimated by 15% [*Prinn et al.*, 1995]. The oceanic sink correspondingly lowers ozone depletion potential estimates for CH_3Br by about one-third from earlier estimates.

TABLE 5.5. Results for Atmospheric and Oceanic CH_3Br From BLAST I and BLAST II Cruises

	BLAST I	BLAST II	Combined Estimate
Global mean (ppt)	9.8	10.4	10.1
NH mean (ppt)	11.2	11.7	11.5
SH mean (ppt)	8.6	9.4	9.0
Variability (ppt)	0.6	1.2	
ITCZ (°N)	4.1	6.4	
IHD (ppt)	2.65	2.31	2.48
NH/SH ratio	1.31	1.25	1.28
SA (%)	-15.7	-19.7	-18.4
P (Gg yr^{-1})	175	248	214
L (Gg yr^{-1}	-188	-267	-229
Net Flux (Gg yr^{-1})	-13.0	-18.7	-14.8

Measured global, northern hemispheric, and southern hemispheric means (NH and SH) and the observed interhemispheric tropical convergence zone (ITCZ), which was used to determine the hemispheric ratios. The net saturation anomaly (SA), the hemispheric ratios, and the interhemispheric difference (IHD) were calculated from the measurements. Finally, estimates of the oceanic production (P), oceanic loss (L), and the net oceanic flux of CH_3Br were added. The net satura-tion anomaly is the percent departure of CH_3Br in the surface ocean from equilibrium with the atmosphere. Negative numbers indicate fluxes from the atmosphere to the ocean. Variability is the residual standard deviation of a loess fit through all atmospheric measurements.

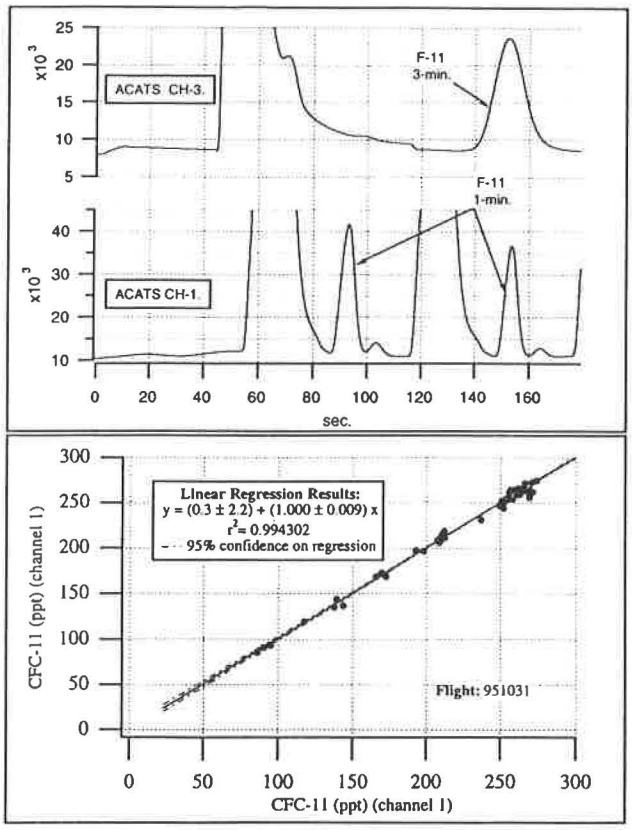

Fig. 5.24. Simultaneous 1- and 3-minute chromatograms and a correlation plot of the 1-minute CFC-11 versus the 3-minute CFC-11 data for this flight.

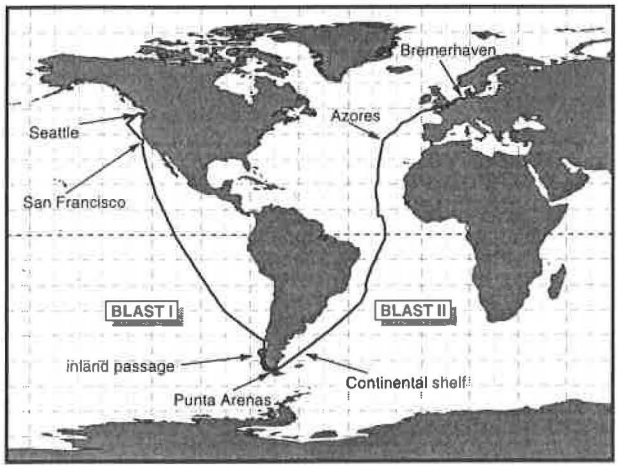

Fig. 5.25. Cruise tracks of both ocean missions. The cruises covered a diverse mixture of coastal waters, upwelling regions, large open ocean areas, and coastally influenced areas in the East Pacific and Atlantic oceans.

Concentrations of CFC-12, CH_3Br, and CH_3Cl in water column samples collected during BLAST II were higher within the mixed layer than at depth. Considering that oceanic CFC-12 originates from the atmosphere, this suggests that both CH_3Br and CH_3Cl have sources associated with the atmosphere or surface waters. Departures of CH_3Br and CH_3Cl concentrations from those of CFC-12 may result from chemical or biological in situ production or degradation of these gases.

Potential artifacts associated with sampling and analysis of CH_3Br and other compounds were investigated. These studies revealed significant problems associated with the measurement of CH_3Br from air stored in stainless steel flasks that have historically been used for measuring CH_3Br in the atmosphere. From a comparison between measurements made shipboard and from air stored in flasks, and from the reanalysis of air in flasks over time, it has been determined that CH_3Br in stainless steel flasks can be unstable and may increase or decrease with time. In addition, results for CH_3Br determined by GC-ECD can be compromised by some GC configurations [*Montzka et al.*, 1995a; *Lobert et al.*, 1996].

Besides CH_3Br, a suite of CFCs and methyl halides was measured during the cruises, and data for oceanic methyl chloride (CH_3Cl), methyl iodide (CH_3I), dibromomethane (CH_2Br_2), and bromoform ($CHBr_3$) are currently being finalized for publication.

5.5. STEALTH PROJECT: AUTOMATED FOUR-CHANNEL FIELD GAS CHROMATOGRAPHS

5.5.1. OVERVIEW

The STEALTH GC was installed at ALT, HFM, ITN, and LEF with different custom configurations for each client. The four-channel STEALTH GC will replace the old HP5920 GCs at the Radiatively Important Trace Species (RITS) stations (BRW, NWR, MLO, SMO, and SPO) and is currently being constructed and laboratory tested.

The data acquisition software and operating system of the STEALTH GC computer is being upgraded. NOAH is currently cooperating with personnel at Harvard University in the development of new data acquisition software for the PC-based UNIX operating system, QNX. QNX is a multitasking and multi-user operating system that will facilitate data acquisition, data retrieval, data archival, and real-time display. The airborne GC, ACATS-IV, is currently being configured to test the QNX data acquisition software. In 1996, NOAH scientists will implement the software on an ACATS-IV deployment and on the new STEALTH station GCs.

The STEALTH GC is an ECD/GC system based on technology developed on ACATS-IV and LACE. The first channel encompasses a Shimadzu mini-2E ECD and a Porapak Q packed column (Figure 5.28). This channel allows for the measurement of N_2O and SF_6. Channel two of the instrument uses a Valco ECD along with a Unibeads 2S packed column. This configuration is capable of measuring N_2O, CFC-12, H-1211, CFC-11, and CFC-113. The third channel also uses a Valco ECD and an OV-101 packed column and is used to measure CFC-11, CFC-113, $CHCl_3$, CH_3CCl_3, CCl_4, and C_2Cl_4 (perchloro-

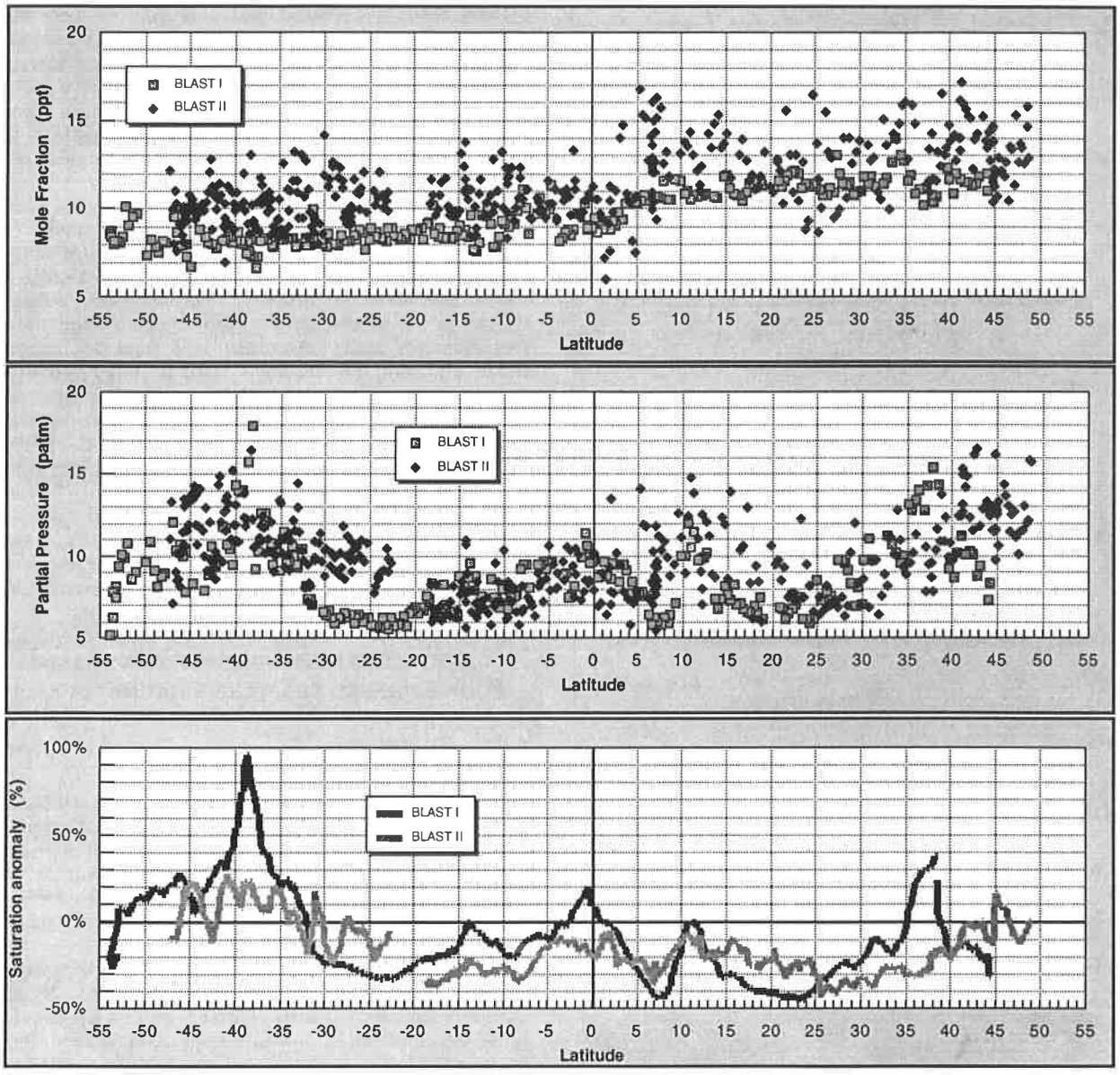

Fig, 5.26 Atmospheric CH_3Br, its partial pressure in the surface water, and the net saturation anomalies for both cruises.

ethylene, PCE). All of the aforementioned channels have been proven in other similar instruments that have been constructed and deployed to various sites.

Channel four, however, has just recently been developed and uses quite a different setup than the other three channels. This channel also uses a Valco ECD, but incorporates a GS Q capillary column rather than a packed column. This channel also uses a Neslab cryocooler which allows for the preconcentration trapping of the three trace gasses, HCFC-22, CH_3Cl, and CH_3Br being measured. With the current configuration of this channel, one is capable of measurements of better than 1% for HCFC-22, 0.5% for CH_3Cl, and 2% for CH_3Br. Figure 5.28d is a chromatogram of the newly developed fourth channel.

5.5.2. Tower GC at WITN in Cooperation with CCG

The GC and instruments that monitor CO_2 and ^{222}Rn are housed in a building adjacent to a tall tower (WITN) in rural North Carolina. Diaphragm pumps located in the building continuously draw air from 51, 123, and 496 m above ground through 1 cm i.d. Dekabon tubing affixed to the tower. Detailed descriptions of sample handling and drying, and initial results of CO_2 measurements at WITN were published [*Bakwin et al.*, 1995]. GC analyses of air from each sampling level and of two calibrated whole-air standards are performed hourly. Standards are stored at high pressure in "Aculife"-treated aluminum cylinders.

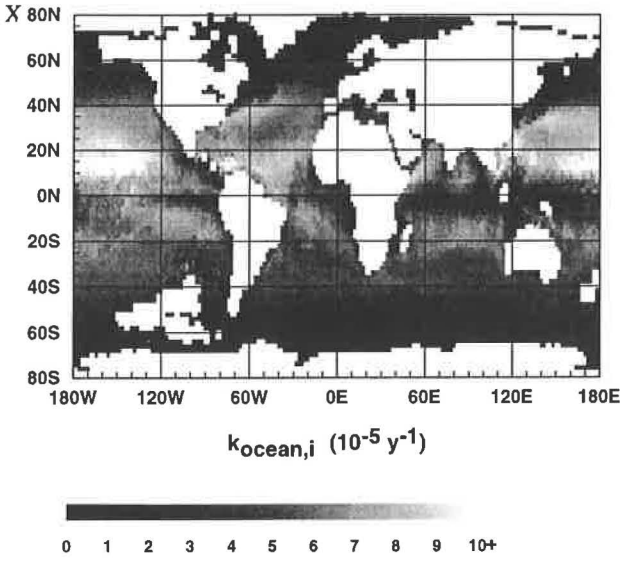

Fig. 5.27. Map of the global distribution of the rate constant ($k_{ocean,\ I}$) for the irreversible uptake of atmospheric methyl bromide (CH_3Br) by the ocean ($k_{ocean,\ I} = 1/\tau_{ocean,\ I}$; global τ_0 = 2.7 years). This rate constant is computed with data from COADS for each cell on a 2° × 2° grid. Note that higher loss rates are found in the northern hemisphere in regions containing both high wind speeds and warm SST's.

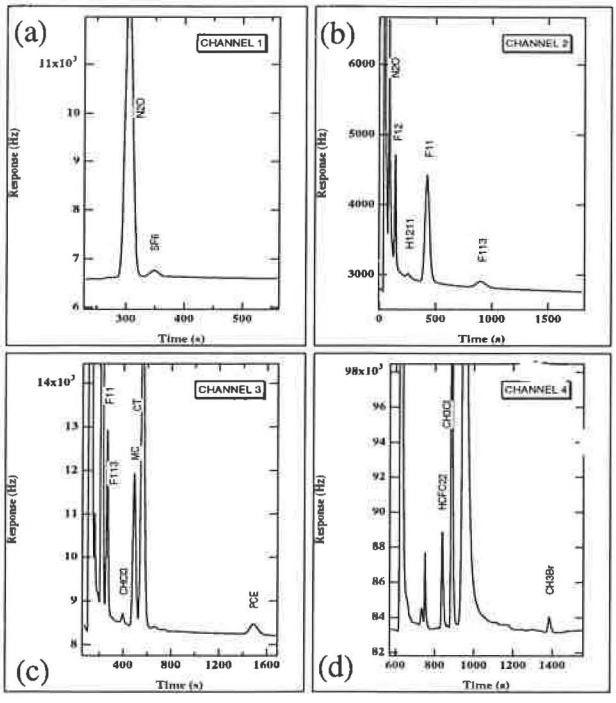

Fig. 5.28. Chromatograms of all four channels of the STEALTH GC that will replace the old RITS HP5890 GCs.

Chromatographic and housekeeping data are logged by a 486SX PC and archived on 1.2 Gb optical disks that are sent to the NOAH laboratory each week for analysis. Instruments and gas supplies are maintained by a technician who visits the site weekly .

Monthly statistics of mixing ratios for several halocompounds and N_2O at the WITN tower are presented in Figure 5.29. Statistics for each sampling height (51, 123, and 496 m) are denoted by 1, 2, and 3, respectively, along the bottom of each plot . For each month, the mean (circle) and standard deviation (distance between circle and asterisk) of the mixing ratios of each species generally decrease with increasing sample height. Variability in trace gas mixing ratios within the continental boundary layer is determined by sources, sinks, boundary layer dynamics, and horizontal transport. Since each species plotted in Figure 5.29 has solely ground-based sources, it is expected that mixing ratios and variability should be greatest near the ground. This effect is inflated at night by the accumulation of emissions from local, ground-based sources in the shallow nocturnal stable layer.

Figure 5.30 gives statistics for the 51-496 m mixing ratio gradients, binned by hour of day, of N_2O, CH_3CCl_3, and SF_6 for November 1995. Significant vertical gradients of N_2O and CH_3CCl_3 were observed at night, indicating these compounds were emitted by local, ground-based sources. In contrast, the insignificant accumulation of SF_6 in the nocturnal stable layer suggests an absence of local, ground-based sources. During the late morning and afternoon, convection rapidly mixes air from the ground to >500 m, and vertical gradients approach zero.

In studying regional emissions of trace gases, it is critical that the influences of local sources are minimized. At WITN, the boundary layer height during the night is typically <500 m. Hence, mixing ratio variability at 496 m during the nighttime is primarily driven by horizontal transport of polluted air to the site, and mixing ratios of long-lived species should reflect regional-scale emissions. Figure 5.31 shows the correlation of CH_3CCl_3 and C_2Cl_4 mixing ratios at 496 m between 2200-0900 EST during November 1995. An orthogonal distance regression through the data yields a slope of 0.62, which can be taken as the regional emission ratio of these two compounds. Using accurate (±5%) estimates of North American emissions of C_2Cl_4 [*McCulloch and Midgely*, 1996], CH_3CCl_3 emissions can be calculated. Using this methodology, emissions of halocompounds, especially those whose production and emissions are controlled by the Montreal Protocol, are monitored.

5.6. Measurement of Air From South Pole Firn

As part of a cooperative venture with scientists from the University of Rhode Island, Pennsylvania State University, and CCG, NOAH analyzed the contents of flasks filled with firn air from the SPO in early 1995 [*Battle et al.*, 1996].

The sampling system was designed so that large quantities of air could be pulled from discrete depths in the firn down to the firn-ice transition depth of 122 m. Because it was possible to obtain large amounts of air, flasks could be flushed adequately and filled for nearly routine air analyses in Boulder and elsewhere. Air at the bottom of the firn had a CO_2 age of about 100 years [*Battle et al.*, 1996].

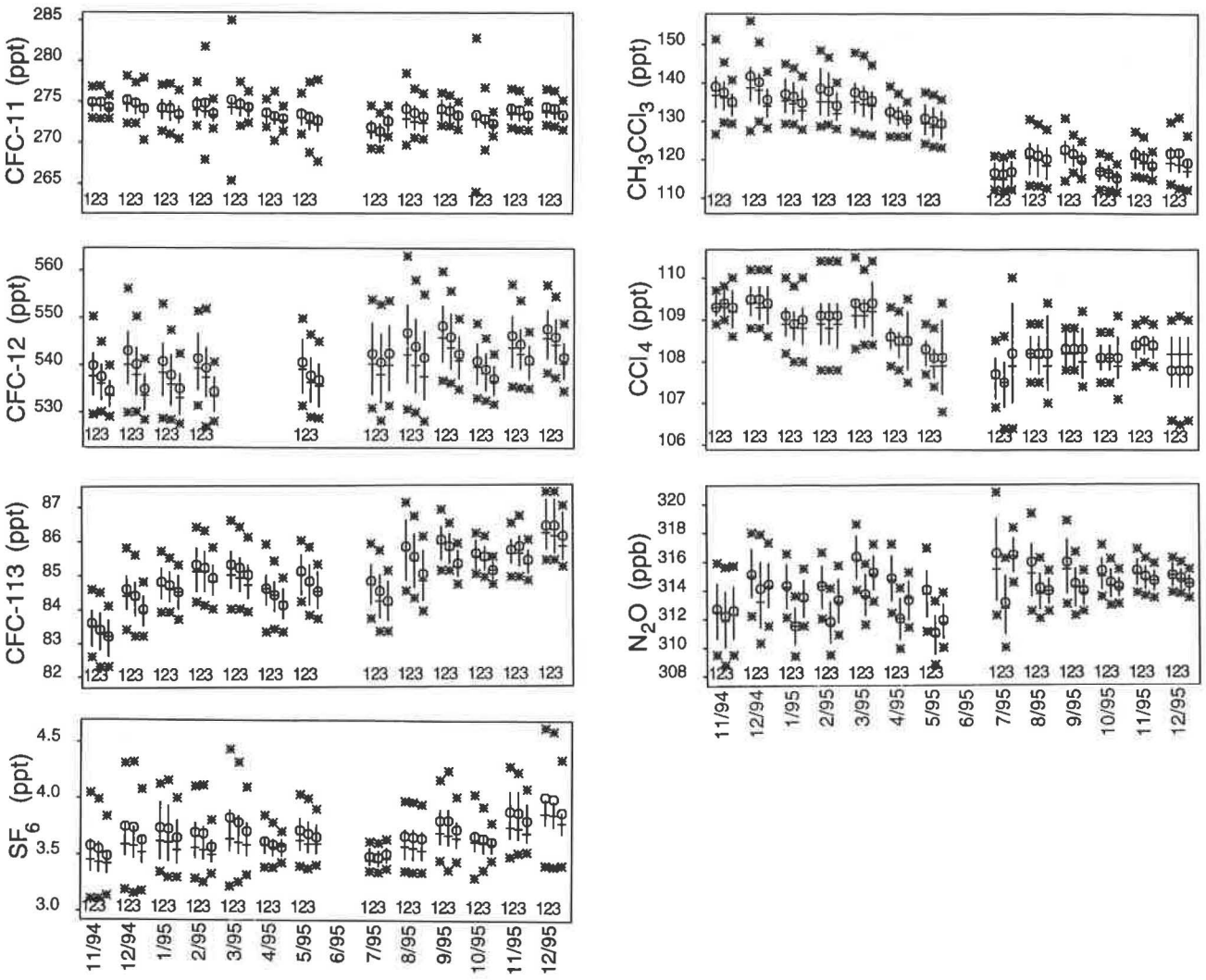

Fig. 5.29. Monthly statistics of CFC-11, CFC-12, CFC-113, methyl chloroform, carbon tetrachloride, nitrous oxide, and sulfur hexafluoride mixing ratios at the WITN tower. Crosses represent medians (horizontal bars) and interquartile range (vertical bars). Circles and asterisks are means and means ±1 standard deviation, respectively. The numbers across the bottom of each plot are the sampling level (1, 2, and 3 refer to 51, 123, and 496 m, respectively).

N_2O in these samples analyzed by NOAH forms a bridge between ice-core data, which typically are much less precise owing to sample handling procedures and small samples, and real-time, present-day measurements (Figure 5.32). These results suggest that preindustrial levels of N_2O in the atmosphere had to be about 280 ppb and that N_2O was increasing steadily through the latter part of the 20th century. The growth rate of atmospheric N_2O from 1904 through 1958 was $0.06 \pm 0.01\%$ yr^{-1} (95% confidence level); thereafter, it has increased at a rate of $0.22 \pm 0.02\%$ yr^{-1} (95% C.L.). N_2O covaried well with CO_2 throughout the profile, although the smoothness of the fit could be attributable to subsurface diffusion of the gases. Nevertheless, the overall trend of N_2O as a function of CO_2 was 0.50 ± 0.03 ppb N_2O ppm^{-1} CO_2^{-1} (95% confidence level, $r^2 = 0.98$).

Surprisingly these flasks, which were sealed with Teflon o-rings, did not cause significant contamination of most halocarbons. Consequently, depth profiles were obtained of CFCs, chlorocarbons, and bromocarbons representing air as far back as the late 19th century. (Dates assigned to halocarbons will be older than CO_2 in the same bolus of air owing to their slower rates of diffusion.) As shown in Figure 5.33, which is a close-up of the lower portion of the CFC-11 profile, the sampling and analytical precisions are on the order of tenths of a ppt. Small amounts of contamination are suggested in that the lowest values were still 2 ppt (<1% of today's atmosphere) and that two pairs of flasks showed higher levels of CFC-11 in some of the deepest firn. This latter contamination was probably caused by stress on the pump near the firn-ice transition zone where less air was available to pull, thus increasing

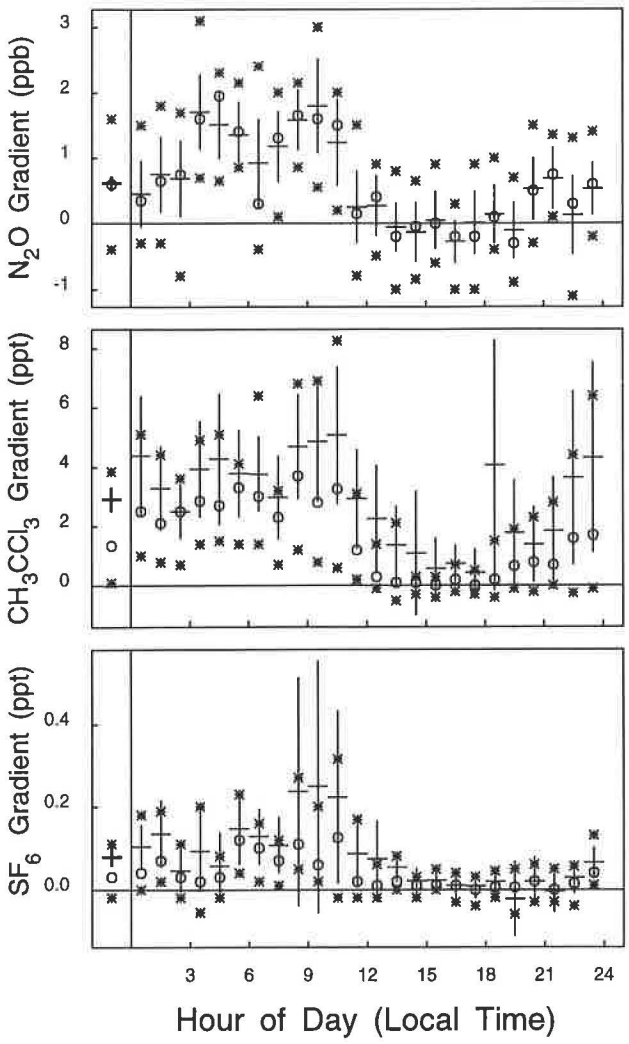

Fig. 5.30. Statistics of 51 m - 496 m mixing ratio gradients for N_2O, CH_3CCl_3, and SF_6, binned by hour, for November 1995. Crosses indicate means (horizontal bars) ± the 95% confidence interval (vertical bars). Circles represent medians, and asterisks indicate upper and lower quartiles. The left panel gives statistics of 51 m - 496 m gradients for the entire month.

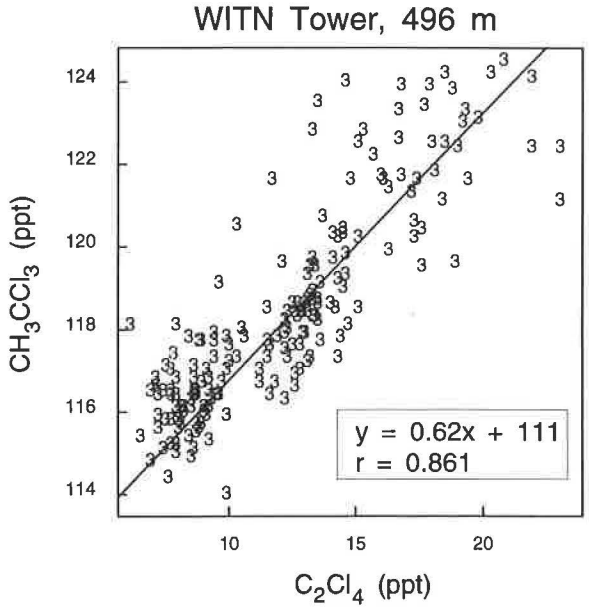

Fig, 5.31. Correlation between CH_3CCl_3 and C_2Cl_4 mixing ratios at 496 m between 2200 and 0900 (EST) during November 1995. The slope of an orthogonal distance regression (0.62) is taken as the regional emission ratio of these two compounds.

the probability of sucking in unrepresentative air. This feature showed up in all of the gases, further suggesting contamination with modern air. Nevertheless, this level of contamination is not representative of the rest of the profile. Thus, we were able to obtain precise, but probably accurate, measurements at sub-ppt levels throughout most of the profile.

These results yield entire atmospheric histories for CFCs, halons, and other halocarbons of purely anthropogenic origin (Figures 5.33 through 5.37). They also showed atmospheric trends for gases of both natural and anthropogenic origin, such as CH_3Br, during a time when the human population, its agricultural output, and its industrial activity increased dramatically. These data demonstrate that natural sources of CFCs and halons are minimal at best and most likely nonexistent. Models of

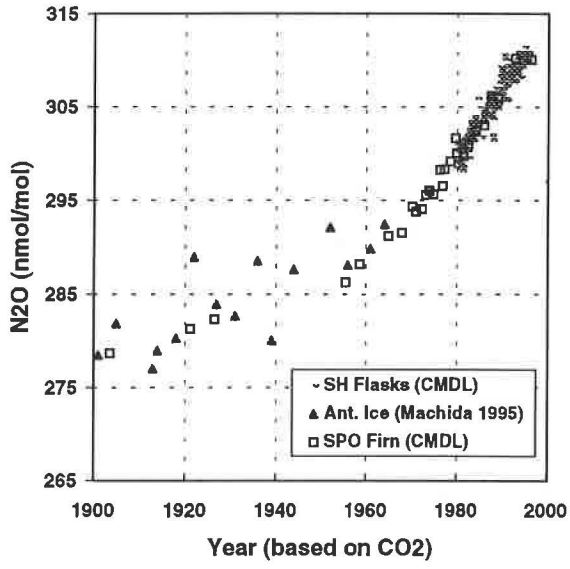

Fig. 5.32. History of atmospheric N_2O over the past century, derived from antarctic ice-core measurements [*Machida et al.*, 1995], real-time air measurements in the southern hemisphere (NOAH), and analyses of South Pole firn air (NOAH). Firn air ages are determined from correlation of CO_2 in the samples with the atmospheric CO_2 history of *Etheridge et al.* [1996]. Diffusivities of N_2O and CO_2 are assumed to be identical and ice core data of *Machida et al.* [1995] have been lowered by 1 ppb to conform to the CMDL scale.

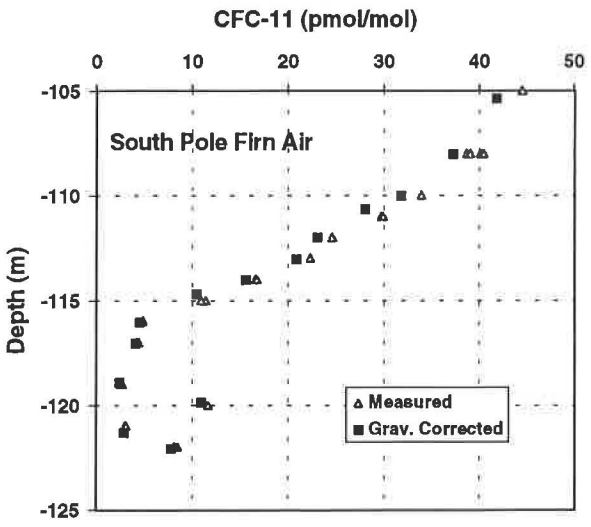

Fig. 5.33. CFC-11 in the lower portion of the firn at the South Pole. The high degree of precision is shown in the actual measurements (triangles), where two flasks were collected at each depth and plotted separately. Only at 108 m depth are these symbols distinguishable and there only because two pairs of flasks from this depth in two separate holes were analyzed. Flasks at 120 and 122 m were subjected to some contamination with modern air during sampling, probably owing to stress on the pump as the firn layers began to turn to ice. Also shown here is the effect of the gravitational correction for settling of CFC-11, which is a gas heavier than air. Again, the error is small.

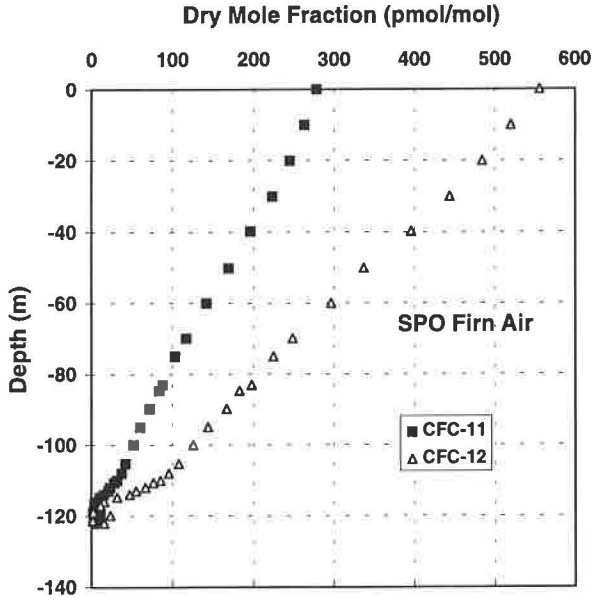

Fig. 5.34. Depth profiles of CFC -11 and -12 in South Pole firn air. Mole fractions of both gases near the bottom of the firn are less than 1% of the present day values, suggesting that natural sources are minimal or non-existent.

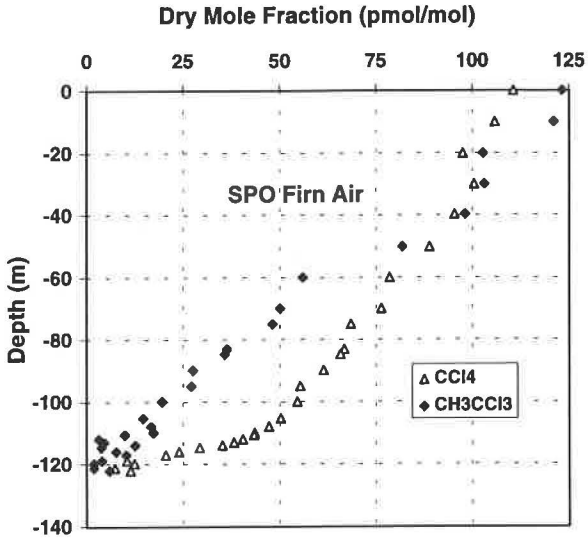

Fig. 5.35. Depth profiles of CCl_4 and CH_3CCl_3 in South Pole firn. There is some evidence of contamination of a few ppt in the CH_3CCl_3 data, although mole fractions of this compound came very close to zero near the bottom of the profile. Mole fractions of CCl_4 never fell below 10 ppt, suggesting either significant, specific contamination of this compound, a very early history of significant anthropogenic release, or a natural source.

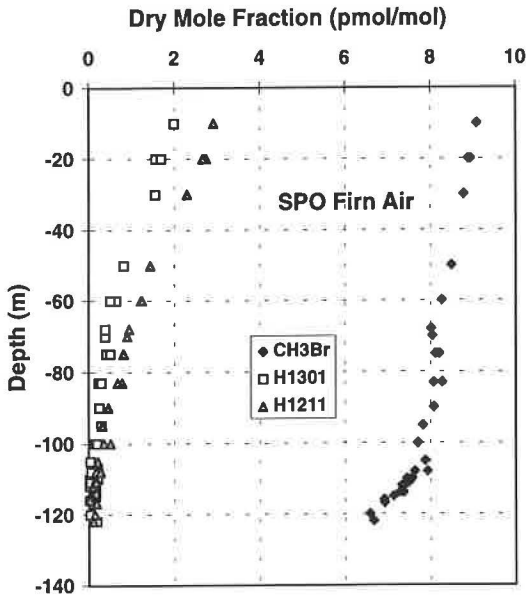

Fig. 5.36. Brominated gases in South Pole firn air. The anthropogenic halon mole fractions both drop to zero early in the profile. These gases were not introduced into the atmosphere in significant amounts until the 1970s. CH_3Br is about 6.5 ppt in air nominally dating back to about 1880.

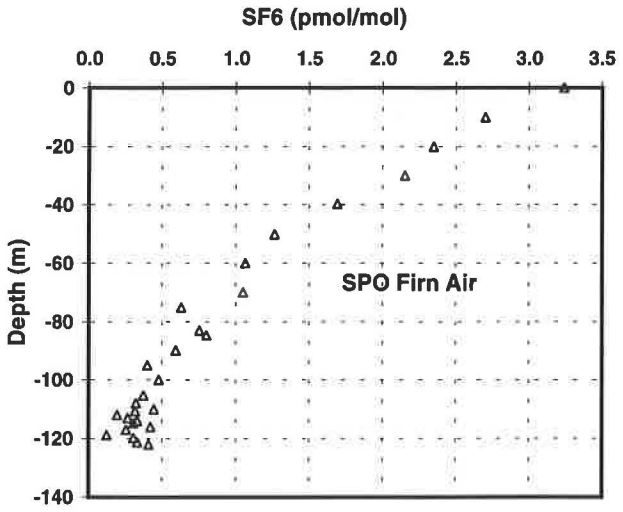

Fig. 5.37. SF_6 in South Pole firn air. Because of its small analytical peak on the GC, the detection limit for SF_6 in real air is around a few tenths of a ppt. Like the halons, this gas was not introduced into the atmosphere until the 1970s [*Maiss et al.*, 1996].

anthropogenic CFC emissions are supported by these findings, confirming the predominance of anthropogenic activity in the atmospheric budget of refractory, organic chlorine. The data for CFCs and the longer-lived organic chlorocarbons ultimately will be useful in dating oceanic water masses and isolated ground waters, providing atmospheric data where none existed before. Atmospheric CH_3Br in the southern hemisphere appears to have been about 25% lower at the turn of the century than it is today (Figure 5.36).

5.7. REFERENCES

AFEAS (Alternative Fluorocarbon Environmental Acceptability Study), *Production, Sales and Atmospheric Release of Fluorocarbons Through 1993*, S & PS, Inc., Washington, D.C., 1995.

Albritton, D.L., R.G. Derwent, I.S.A. Isaken, M. Lal, D.J. Wuebbles, Trace gas radiative forcing indices, in *Climate Change 1994: Radiative Forcing of Climate Change and An Evaluation of the IPCC IS92 Emission Scenarios*, edited by J.T. Houghton, L.G.M. Filho, J. Bruce, H. Lee, B.A. Callander, E. Haites, N. Harris, and K. Maskell, 339 pp., Cambridge University Press, Cambridge, UK, 1995.

Bakwin, P.S., P.P Tans, C. Zhao, W. Ussler, III, and E. Quesnell, Measurements of carbon dioxide on a very tall tower, *Tellus*, 47B, 535-549, 1995.

Battle, M., M. Bender, T. Sowers, P. Tans, J. Butler, J. Elkins, J. Ellis, T. Conway, N. Zhang, P. Lang, and A. Clarke, Histories of atmospheric gases from the firn at South Pole. *Nature*, in press, 1996.

Boering, K.A., E.J. Hintsa, S.C. Wofsy, J.G. Anderson, B.C. Daube, A.E. Dessler, M. Loewenstein, M.P. McCormick, J.R. Podolske, E.M. Weinstock, and G.K. Yue, Measurements of stratospheric carbon dioxide and water vapor at northern midlatitudes: Implications for troposphere-to-stratosphere transport, *Geophys. Res. Lett.*, 22, 2737-2740, 1995.

Butler, J.H., The potential role of the ocean in regulating atmospheric CH_3Br, *Geophys. Res. Lett.*, 21, 185-189, 1994.

Butler, J.H., Methyl bromide under scrutiny. *Nature*, 376, 469-470, 1995.

Butler, J.H., Scientific uncertainties in the budget of atmospheric methyl bromide, *Atmos. Environ.*, 30(7), i-iii, 1996.

Butler, J.H., and J. Rodriguez, Methyl bromide in the atmosphere, in *The Methyl Bromide Issue*, edited by N. Price, London, Wiley and Sons, Ltd., in press, 1996.

Butler, J.H., J.W. Elkins, B.D. Hall, S.O. Cummings, and S.A. Montzka, A decrease in the growth rates of atmospheric halon concentrations, *Nature*, 359, 403-405, 1992.

Butler, J.H., Lobert J.M., S.A. Yvon, and L.S. Geller, The distribution and cycling of halogenated trace gases between the atmosphere and ocean, in *The Expedition Antarktis XII of RV "Polarstern" in 1994/95. Reports of Legs ANT XII/1 and 2*, edited by G. Kattner and K. Fuetterer, Alfred Wegener Institute for Polar and Marine Research, Bremerhaven, 1995.

Daniel, J.S., S. Solomon, and D.L. Albritton, On the evaluation of halocarbon radiative forcing and global warming potentials, *J. Geophys. Res.*, 100, 1271-1285, 1995.

Elkins, J.W., T.M. Thompson, T.H. Swanson, J.H. Butler, B.D. Hall, S.O. Cummings, D.A. Fisher, and A.G. Raffo, Decrease in the growth rates of atmospheric chlorofluorocarbons 11 and 12, *Nature*, 364, 780-783. 1993.

Elkins, J.W., D.W. Fahey, J.M. Gilligan, G.S. Dutton, T.J. Baring, C.M. Volk, R.E. Dunn, R.C. Myers, S.A. Montzka, P.R. Wamsley, A.H. Hayden, J.H. Butler, T.M Thompson, T.H. Swanson, E.J. Dlugokencky, P.C. Novelli, D.F. Hurst, J.M. Lobert, S.J. Cicora, R.J. McLaughlin, T.L. Thompson, R.H. Winkler, P.J. Fraser, L.P. Steele, M.P. Lucarelli, Airborne gas chromatograph for in situ measurements of long lived species in the upper troposphere and lower stratosphere, *Geophys. Res. Lett*, 23(4), 347-350, 1996.

Eluszkiewicz, J., D. Crisp, R. Zurek, L. Elson, E. Fishbein, L. Froidevaux, J. Waters, R.G. Grainger, A. Lambert, R. Harwood, and G. Peckham, Residual circulation in the stratosphere and lower mesosphere as diagnosed from microwave limb sounder data, *J. Atmos. Sci.*, 53, 217-240, 1996.

Etheridge, D.M., L.P. Steele, R.L. Langenfelds, R.J. Francey, J.M. Barnola, and V.I. Morgan, Natural and anthropogenic changes in atmospheric CO_2 over the last 1000 years from air in Antarctic ice and firn. *J. Geophys. Res.*, 101(D2), 4115-4128, 1996.

Fahey, D.W., J.W. Elkins, S.A. Montzka, R.C. Myers, G.S. Dutton, C.M. Volk, Mean age of the air mass: In situ measurements of stratospheric sulfur hexafluoride in 1994, *EOS*, 76, p. 130, 1995.

Fahey, D.W., D.M. Murphy, K.K. Kelly, M.K.W. Ko, M.H. Proffitt, C.S. Eubank, D.W. Ferry, M. Loewenstein, and K.R. Chan, Measurements of nitric oxide and total reactive nitrogen in the Antarctic stratosphere: Observations and chemical implications, *J. Geophys. Res.*, 94, 16,665-16,681, 1989.

Garcia, R.R., and S. Solomon, A New numerical model of the middle atmosphere 2. Ozone and related species, *J. Geophys. Res.*, 99, 12,937-12,951, 1994.

Geller, L., J. Lobert, J. Butler, R. Myers, J. Elkins, Latitudinal distribution of sulfur hexafluoride in and over the Atlantic and E. Pacific Oceans, *EOS*, 76, p. 17, 1994.

Goldan, P.D., W.C. Kuster, D.L. Albritton, and A.L. Schmeltekopf, Stratospheric $CFCl_3$, CF_2Cl_2, and N_2O height profile measurements at several latitudes, *J. Geophys. Res.*, 85, 413-423, 1980.

Hurst, D., L. Geller, P. Novelli, P. Bakwin, R. Myers, J. Elkins, Observations of sulfur hexafluoride from a very tall tower in the southeastern United States, *EOS*, 76, p. 70, 1995.

Hall, T. M., and R. A. Plumb, Age as a diagnostic of stratospheric transport, *J. Geophys. Res.*, 99, 1059-1070, 1994.

Irion, F.W., M. Brown, G.C. Toon, M.R. Gunson, Increase in atmospheric CHF_2Cl (HCFC-22) over Southern California from 1985 to 1990, *Geophys. Res. Lett.*, 21, 1723-1726, 1994.

Lobert, J.M., J.H. Butler, S.A. Montzka, L.S. Geller, R.C. Myers, and J.W. Elkins, A net sink for atmospheric methyl bromide in the East Pacific Ocean. *Science,* 267, 1002-1005, 1995.

Lobert, J. M., J. H. Butler, L. S. Geller, S. A. Yvon, S. A. Montzka, R. C. Myers, A. D. Clarke, J. W. Elkins, BLAST 94: Bromine Latitudinal Air Sea Transect 1994. Report on Oceanic Measurements of Methyl Bromide and Other Compounds, *NOAA Tech. Memo. ERL CMDL-10,* 39 pp., NOAA Environmental Research Laboratories, Boulder, CO, 1996.

Machida, T., T. Nakazawa, Y. Fujii, S. Aoki, and O. Watanabe, Increase in the atmospheric nitrous oxide concentration during the last 250 years, *Geophys. Res. Lett.,* 22(21), 2921-2924, 1995.

Maiss, M., L.P. Steele, R.J. Francey, P.J. Fraser, R.L. Langenfelds, N. B.A. Trivett, and I. Levin, Sulfur hexafluoride—a powerful new atmospheric trace, *Atmos. Environ.*, 30, 1621-1629, 1996.

McCormick, M.P., E.W. Chiou, L.R. McMaster, W.P. Chu, J.C. Larsen, D. Rind, and S. Oltmans, Annual variations of water vapor in the stratosphere and upper troposphere observed by the Stratospheric Aerosol and Gas Experiment II, *J. Geophys. Res.*, 98, 4867-4874, 1993.

McCulloch, A., and P. Midgely, The production and global distribution of emissions of trichloroethene, tetrachloroethene, and dichloromethane over the period 1988-1992, *Atmos. Env.,* 30, 601-608, 1996.

McElroy, M. B., R. J. Salawitch, S. C. Wofsy and J. A. Logan, Reductions of antarctic ozone due to synergistic interactions of chlorine and bromine, *Nature,* 321, 759-762, 1986.

Minschwaner, K., R.J. Salawitch, and M.B. McElroy, Absorption of solar radiation by O_2: Implications for O_3 and lifetimes of N_2O, $CFCl_3$, and CF_2Cl_2, *J. Geophys. Res.*, 98, 10,543-10,561, 1993.

Montzka, S.A., R.C. Myers, J.H. Butler, J.W. Elkins, and S.O. Cummings, Global tropospheric distribution and calibration scale of HCFC-22, *Geophys. Res. Lett.,* 20, 703-706, 1993.

Montzka, S.A., R.C. Myers, J.H. Butler, and J.W. Elkins, Early trends in the global tropospheric distribution of hydrofluorocarbon-141b and -142b, *Geophys. Res. Lett.,* 21, 2483-2486, 1994.

Montzka, S.A., J.H. Butler, J.W. Elkins, S. Yvon, A. Clarke, J. Lobert, and L. Lock, Difficulties associated with measuring atmospheric levels of methyl bromide and other methyl halides, *EOS,* 76, S160, 1995a.

Montzka, S.A., R.C. Myers, J.M. Butler, T.M. Thompson, J.W. Elkins, L.T. Lock, A.D. Clarke, T.H. Swanson, Changing trends in the global tropospheric abundance of CFCs, HCFC, HFCs, and chlorine in recent time, *EOS,* 76, F98, 1995b.

Montzka, S.A., R.C. Myers, J.H. Butler, J.W. Elkins, L.T. Lock, A.D. Clarke, A.H. Goldstein, Observations of HFC-134a in the remote troposphere, *Geophys. Res. Lett.,* 23, 169-172, 1996a.

Montzka, S.A., J.H. Butler, R.C. Myers, T.M. Thompson, T.H. Swanson, S.D. Clarke, L.T. Lock, J.W. Elkins, Decline in the tropospheric abundance of halogen from halocarbons, *Science,* 272, 1318-1322, 1996b.

Mote, P.W., K.H. Rosenlof, M.E. McIntyre, E.S. Carr, J.S. Kinnersley, H.C. Pumphrey, R.S. Harwood, J.R. Holton, J.M. Russell III, J.W. Waters, J.C. Gille, and K.K. Kelly, An atmospheric tape recorder: The imprint of tropical tropopause temperatures on stratospheric water vapor, *J. Geophys. Res.*, 101, 3989-4006, 1996.

Murphy, D.M., S.W. Fahey, M.H. Proffitt, S.C. Liu, K.R. Chan, C.S. Eubank, S.R. Kawa, and K.K. Kelly, Reactive nitrogen and its correlation with ozone in the lower stratosphere and upper troposphere, *J. Geophys. Res.*, 98, 8751-8773, 1993.

Oram, D.E., C.E. Reeves, S.A. Penkett, and P.J. Fraser, Measurements of HCFC-142b and HCFC-141b in the Cape Grim air archive: 1978-1993, *Geophys. Res. Lett.,* 22, 2741-2744, 1995.

Peterson, J.T., and R.M. Rosson (Eds.), *Climate Monitoring and Diagnostics Laboratory, No. 21, Summary Report 1992*, 131 pp., NOAA Environmental Research Laboratories, Boulder, CO, 1993.

Peterson, J.T., and R.M. Rosson (Eds.), *Climate Monitoring and Diagnostics Laboratory, No. 22, Summary Report 1993*, 152 pp., NOAA Environmental Research Laboratories, Boulder, CO, 1994.

Plumb, R.A., A "tropical pipe" model of stratospheric transport, *J. Geophys. Res.*, 101, 3957-3972, 1996.

Plumb, R.A., and M.K.W. Ko, Interrelationships between mixing ratios of long-lived stratospheric constituents, *J. Geophys. Res., 97,* 10,145-10,156, 1992.

Podolske, J., and M. Loewenstein, Airborne tunable diode laser spectrometer for trace-gas measurement in the lower stratosphere, *Appl. Opt.*, 32, 5324-5333, 1993.

Pollock, W.H., L.E. Heidt, R.A. Lueb, J.F. Vedder, M.J. Mills, S. Solomon, On the age of stratospheric air and ozone depletion potentials in polar regions, *J. Geophys. Res.,* 97, 12,993-12,999, 1992.

Prather, M.J., and R.T. Watson, Stratospheric ozone depletion and future levels of atmospheric chlorine and bromine, *Nature,* 344, 729-734, 1990.

Prinn, R.G., R.F. Weiss, B.R. Miller, J. Huang, F.N. Alyea, D.M. Cunnold, P.J. Fraser, D.E. Hartley, and P.G. Simmonds, Atmospheric trends and lifetime of CH_3CCl_3 and global OH concentrations, *Science,* 269, 187-192, 1995.

Proffitt, M.H., and J. McLaughlin, Fast-response dual-beam UV absorption ozone photometer suitable for use on stratospheric balloons, *Rev. Sci. Instrum.*, 54, 1719-1728, 1983.

Randel, W.J., J.C. Gille, A.E. Roche, J.B. Kumer, J.L. Mergenthaler, J.W. Waters, E.F. Fishbein, and W.A. Lahoz, Stratospheric transport from the tropics to middle latitudes by planetary-wave mixing, *Nature,* 365, 533-535, 1993.

Ravishankara, A. R., S. Solomon, A.A. Turnipseed, R.F. Warren, Atmospheric lifetimes of long-lived halogenated species, *Science,* 259, 194-199, 1993.

Rinsland, C. P., E. Mahieu, R. Zander, M. R. Gunson, R. J. Salawitch, A. Y. Chang, A. Goldman, M. C. Abrams, M. M. Abbas, M. J. Newchurch, and F. W. Irion, Trends of OCS, HCN, SF_6, and $CHClF_2$ (HCFC-22) in the lower stratosphere from 1985 and 1994 atmospheric trace molecule spectroscopy experiment measurements near 30°N latitude, *Geophys. Res. Lett.,* in press, 1996.

Rosenlof, K.H., Seasonal cycle of the residual mean meridional circulation in the stratosphere, *J. Geophys. Res.*, 100, 5173-5191, 1995.

Salawitch, R.J., S.C. Wofsy, P.O. Wennberg, R.C. Cohen, J.G. Anderson, D.W. Fahey, R.S. Gao, E.R. Keim, E.L. Woodbridge, R.M. Stimpfle, J.P. Koplow, D.W. Kohn, C.R. Webster, R.D. May, L. Pfister, E.W. Gottlieb, H.A. Michelsen, G.K. Yue, M.J. Prather, J.C. Wilson, C.A. Brock, H.H. Jonsson, J.E. Dye, D. Baumgardner, M.H. Proffitt, M. Loewenstein, J.R. Podolske, J.W. Elkins, G.S. Dutton, E.J. Hintsa, A.E. Dessler, E.M. Weinstock, K.K. Kelly, K.A. Boering, B.C. Daube, K.R. Chan, and S.W. Bowen, The diurnal variation of hydrogen, nitrogen, and chlorine radicals: Implications for the heterogeneous production of HNO_2, *Geophys. Res. Lett.*, 21, 2251-2554, 1994.

Schauffler S.M., L.E. Heidt, W.H. Pollock, T.M. Gilpin, J.F. Vedder, S. Solomon, R.A. Lueb, and E.L. Atlas, Measurements of halogenated organic compounds near the tropical tropopause, *Geophys. Res. Lett.*, 22, 2567-2570, 1993.

Schauffler S.M., W.H. Pollock, E.L. Atlas, L.E. Heidt, and J.S. Daniel, Atmospheric distributions of HCFC 141b, *Geophys. Res. Lett.*, 22, 819-822, 1995.

Shorter, J.H., C.E. Kolb, P.M. Crill, R.A. Kerwin, R.W. Talbot, M.E. Hines, and R.C. Harriss, Rapid degradation of atmospheric methyl bromide in soils. *Nature,* 377, 717-719, 1995.

Solomon S., R. W. Portmann, R. R. Garcia, L. W. Thomason, L.R. Poole, and M. P. McCormick, The role of aerosol variations in anthropogenic ozone depletion at northern midlatitudes, *J. Geophys. Res.*, 101, 6713-6727, 1996.

Stolarski, R.S., S.L. Baughcum, W.H. Brune, A.R. Douglass, D.W. Fahey, R.R. Friedl, S.C. Liu, R.A. Plumb, L.R. Poole, H.L. Wesoky, D.R. Worsnop, 1995 Scientific Assessment of the Atmospheric Effects of Stratospheric Aircraft, *NASA Ref. Pub. 1381*, 1996.

Swanson, T.H., J.W. Elkins, J.H. Butler, S.A. Montzka, R.C. Myers, T.M. Thompson, T.J. Baring, S.O. Cummings, G.S. Dutton, A.H. Hayden, J.M. Lobert, G.A. Holcomb, W.T. Sturges, and T.M. Gilpin, in Climate Mo*nitoring and Diagnostics Laboratory No. 21 Summary Report 1992*, edited by J.T. Peterson and R.M. Rosson, pp. 59-75, NOAA Environmental Research Laboratories, Boulder, CO, 1993.

Thompson, T.M., J.W. Elkins, J.H. Butler, S.A. Montzka, R.C. Myers, T.J. Baring, S.O. Cummings. G.S. Dutton, J.M Gilligan, A.H. Hayden, J.M. Lobert, T.H. Swanson, D.F. Hurst, and C.M. Volk, in *Climate Monitoring and Diagnostics Laboratory No. 22 Summary Report 1992*, pp. 72-91, edited by J.T. Peterson and R.M. Rosson, NOAA Environmental Research Laboratories, Boulder, CO, 1994.

Trepte, C.R., and M.H. Hitchman, Tropical stratospheric circulation deduced from satellite aerosol data, *Nature*, 355, 626-628, 1992.

Volk, C.M., J.W. Elkins, D.W. Fahey, R.J. Salawitch, G.S. Dutton, J.M. Gilligan, M.H. Proffitt, M. Loewenstein, J.R. Podolske, K. Minschwaner, J.J. Margitan, and K.R. Chan, Quantifying transport between the tropical and midlatitude lower stratosphere, *Science*, 272, 1763-1768, 1996.

WMO (World Meteorological Organization), *Scientific Assessment of Ozone Depletion: 1994*, WMO, Geneva, 1995.

Yung, Y.L., J.P. Pinto, R.T. Watson and S.P. Sander, Atmospheric bromine and ozone perturbations in the lower stratosphere, *J. Atmos. Sci.*, 37, 339-353, 1980.

Yvon, S.A., and J.H. Butler An improved estimate of the oceanic lifetime of atmospheric CH_3Br, *Geophys. Res. Lett.*, 23, 53-56, 1996.

Zander, R., E. Mahieu, P. Demoulin, C.P. Rinsland, D.K. Weisenstein, M.K.W. Ko, N.D. Sze, and M.R. Gunson, Secular evolution of the vertical column abundances of $CHClF_2$ (HCFC-22) in the Earth's atmosphere inferred from ground-based IR solar observations at the Jungfraujoch and at Kitt Peak, and comparison with model calculations, *J. Atmos, Chem*, 18, 129-148, 1994.